T.R.
ONDOKUZ MAYIS UNIVERSITY
INSTITUTE OF GRADUATE STUDIES
DEPARTMENT OF CHEMICAL ENGINEERING

INVESTIGATION OF THE EFFECT OF CATALYST SUPPORT MATERIALS ON OLEIC ACID CATALYTIC DEOXYGENATION

Master's Thesis

Mohammed Siraj ESHETEA

Supervisor

Prof. Dr. Selim CEYLAN

SAMSUN
2022

T.R.
ONDOKUZ MAYIS UNIVERSITY
INSTITUTE OF GRADUATE STUDIES
DEPARTMENT OF CHEMICAL ENGINEERING

INVESTIGATION OF THE EFFECT OF CATALYST SUPPORT MATERIALS ON OLEIC ACID CATALYTIC DEOXYGENATION

Master's Thesis

Mohammed Siraj ESHETEA

Supervisor

Prof. Dr. Selim CEYLAN

SAMSUN
2022

ACCEPTANCE AND APPROVAL OF THE THESIS

The study entitled **"INVESTIGATION OF THE EFFECT OF CATALYST SUPPORT MATERIALS ON OLEIC ACID CATALYTIC DEOXYGENATION"** prepared by **Mohammed Siraj ESHETEA** and supervised by **Prof. Dr. Selim CEYLAN** was found successful and unanimously accepted by committee members as MSc thesis of the Department of Chemical Engineering, following the examination on the date 23/08/2022.

	Title Name Surname **University** **Department**	**Signature**	**Final decision**
Chairman	Dr. Öğr. Üyesi Kamil Serkan UZYOL İstanbul Nişantaşı University Department of Nutrition and Dietetics		☒Accept ☐ Reject
Member	Prof. Dr. Selim CEYLAN Ondokuz Mayis University Department of Chemical Engineering		☒Accept ☐ Reject
Member	Dr. Öğr. Üyesi Berker FIÇICILAR Ondokuz Mayis University Department of Chemical Engineering		☒Accept ☐ Reject

This thesis has been approved by the committee members that already stated above and determined by the Institute Executive Board.

APPROVAL
... / ... /2022
Prof. Dr. Ali BOLAT
Head of Institute of Graduate Studies

DECLARATION OF COMPLIANCE WITH SCIENTIFIC ETHIC

I hereby declare and undertake that I complied with scientific ethics and academic rules in all stages of my MSc thesis, that I have referred to each quotation that I use directly or indirectly in the study and that the works I have used consist of those shown in the sources, that it was written in accordance with the institute writing guide and that the situations stated in the article 3, section 9 of the Regulation for TÜBİTAK Research and Publication Ethics Board were not violated.

Is Ethics Committee Necessary?

Yes ☐ (If it necessary, please add appendices.)

No ☒

Signature
27/06/2022
Mohammed Siraj ESHETEA

DECLARATION OF THE THESIS STUDY ORIGINALITY REPORT

Thesis Title: INVESTIGATION OF THE EFFECT OF CATALYST SUPPORT MATERIALS ON OLEIC ACID CATALYTIC DEOXYGENATION

As a result of the originality report taken by me from the plagiarism detection program on 27/06/2022 for the thesis titled above;

Similarity ratio : % 21

Single resource rate : % 3 has been released.

Signature
27/06/2022
Prof. Dr. Selim CEYLAN

ÖZET

KATALIZÖR DESTEK MALZEMELERININ OLEIK ASIT KATALITIK DEOKSIJENASYONU ÜZERINE ETKISININ İNCELENMESI

Mohammed Siraj ESHETEA
Ondokuz Mayıs Üniversitesi
Lisansüstü Eğitim Enstitüsü
Kimya Mühendisliği Anabilim Dalı
Yüksek Lisans, Haziran/2022
Danışman: Prof. Dr. Selim CEYLAN

Bazı oksijenli türlerin varlığı nedeniyle, geleneksel biyodizelin yerini almak üzere oksijensizleştirme (DO) teknolojisinden elde edilen yeşil dizel geliştirilmiştir. Çalışma, desteklerin CoMo katalizörü kullanılarak oleik asidin deoksijenasyonu üzerindeki etkilerine odaklanmıştır. Bu çalışmanın sonuçları, Molibden ve kobalt türlerinin ürünün reaktivitesi ve dağılımı üzerinde önemli bir etkiye sahip olduğunu ortaya koymuştur. Seryum oksit (CeO_2), Titanyum dioksit (TiO_2), aktif karbon (AC), Zeolit ve Alüminyum oksit (γ-Al_2O_3) üzerinde desteklenen CoMo bazlı katalizör, ıslak emprenyasyon yöntemi ile hazırlanmış ve ardından 550 °C sıcaklıkta 4 saat boyunca 20 mL dk^{-1} N_2 akış altında kalsine edilmiştir. Hazırlanan katalizörler, X-ışını kırınımı (XRD), Brunauer-Emmett- Teller (BET), Termo-Gravimetrik Analiz (TGA) ve Taramalı Elektron Mikroskobu (SEM) analizi ile karakterize edilmiştir. Destek tipinin etkisi (Aktif karbon, γ-Al_2O_3, CeO_2, TiO_2, ve Zeolit), 350 °C'de ve atmosfer basıncında desteklenen CoMo katalizörleri üzerinde oleik asidin deoksijenasyonunda farklı oksijenli fonksiyonel grupların uzaklaştırılması konusunda araştırılmıştır. Oksijeni giderilmiş sıvı ürünler, Fouriertransform kızılötesi spektroskopisi (FTIR), Gaz Kromatografisi-Kütle Spektrometrisi (GC-MS), Yüksek ısıtma değeri (HHV) ve CHNOS analizi ile karakterize edilmiştir. Olası bir alternatif süreç simülasyonu geliştirmek için kütle ve enerji dengesini, sermaye yatırımını ve yeşil dizel üretimi için tesisin üretim maliyetini tahmin etmek için SuperPro tasarım v9.0 kullanılarak gerçekleştirilmiştir. Çalışma sonuçlarına göre CoMo/AC, 350 °C'de 2 saat boyunca %93,20 hidrokarbon verimi ile en aktif katalizördür olup hidrojen yokluğunda 300 rpm'de. Bununla birlikte, γ-Al_2O_3, CeO_2, TiO_2 ve zeolit üzerinde destekli CoMo katalizörler için önemli bir deoksijenasyon reaksiyonu hala gözlenmiştir. Genel olarak, CoMo/AC, iyi fizikokimyasal özelliklerinden dolayı iyi katalitik performans gösterilmiştir.

Anahtar Kelimeler: Oksijensizleştirme, SuperPro tasarımı, Yeşil dizel, Oleik asit, Zeolit.

ABSTRACT

INVESTIGATION OF THE EFFECT OF CATALYST SUPPORT MATERIALS ON OLEIC ACID CATALYTIC DEOXYGENATION

Mohammed Siraj ESHETEA
Ondokuz Mayıs University
Institute of Graduate Studies
Department of Chemical Engineering
Master, June/2022
Supervisor: Prof. Dr. Selim CEYLAN

Due to the presence of certain oxygenated species, green diesel from deoxygenation (DO) technology was developed to replace conventional biodiesel. The study focused on the effects of the supports on the deoxygenation of oleic acid using the CoMo catalyst. The results of this study revealed that the Molybdenum and cobalt species have a significant influence on the reactivity and distribution of the product. The CoMo-based catalyst supported on Cerium oxide (CeO_2), Titanium dioxide (TiO_2), activated carbon (AC), Zeolite, and Aluminum oxide (γ-Al_2O_3) were prepared by wet impregnation method and then calcinated under 20 mL min^{-1} N_2 flow for 4 hours at a temperature of 550 °C. The prepared catalysts were characterized by X-ray diffraction (XRD), Brunauer-Emmett-Teller (BET), Thermo-Gravimetric Analysis (TGA), and Scanning Electron Microscopy (SEM) analysis. The effect of support type (Active carbon, γ-Al_2O_3, CeO_2, TiO_2, and Zeolite) on the removal of the different oxygenated functional groups was investigated in the deoxygenation of oleic acid over supported CoMo catalysts at 350 °C and atmospheric pressure. The deoxygenated liquid products were characterized by Fourier-transform infrared spectroscopy (FTIR), Gas Chromatography-Mass Spectrometry (GC-MS), Higher heating value (HHV), and CHNOS analysis. To develop a possible alternative process simulation was conducted using SuperPro design v9.0 to estimate the mass and energy balance, capital investment, and the production cost of the plant for the production of green diesel. Based on the study results, CoMo/AC is the most active catalyst with 93.20% hydrocarbon yield for 2 hrs. at 350 °C and 300 rpm in the absence of hydrogen. However, a significant deoxygenation reaction was still observed for the catalysts having CoMo supported on γ-Al_2O_3, CeO_2, TiO_2, and zeolite. Overall, The CoMo/AC shows good catalytic performance due to its good physicochemical properties.

Keywords: Deoxygenation, SuperPro design, Green diesel, Oleic acid, Zeolite.

ACKNOWLEDGEMENT

First of all, I would like to give glory to the Almighty Allah, who reigns forever. Because he is the one who provided me with good health and capacity throughout this study. I’m also grateful to my advisor, Prof. Dr. Selim Ceylan, for his priceless motivation and advice that helped me to complete this thesis. The words he used and the approach he showed me made me more confident in myself throughout our journey.

My special thanks to Dr. Burak Tekin, Arş. Gör. Gülce Çakman and Arş. Gör. Rukan Can Seyfeli encouraged me throughout my thesis. They contributed much with their thoughtful insights and helpful feedback to the study. I would also like to thank all the staff workers in the Chemical Engineering department, for providing their help when I needed it and for making my stay comfortable.

My heartfelt gratitude goes to the Presidency for Turks Abroad and Related Communities for facilitating my scholarship to pursue my studies in Turkey. Lastly, I thank my family for their consistent prayers and support.

Mohammed Siraj ESHETEA

CONTENTS

SYMBOLS AND ABBREVIATIONS

AC	: activated carbon
AHMT	: Ammonium heptamolybdate
Al_2O_3	: Aluminum oxide
AOC	: Annual operating cost
BET	: Brumaire-Emmett-Teller
BJH	: Barrett-Joyner-Halenda analysis
C	: Carbon
CeO_2	: Cerium oxide
CFC	: Contractor's fee & contingency
CHNOS	: Elemental analysis
CNHH	: Cobalt (II) nitrate hexahydrate
CO	: Carbon mono oxide
Co	: Cobalt
CO_2	: Carbon dioxide
CoMo	: Cobalt and Molybdenum
Cv	: Heat capacity
deCOx	: Decarboxylation
DFC	: Direct fixed capital cost
DO	: Deoxygenation
EDX	: Energy dispersive X-ray
SEM	: Scanning electron microscope
FTIR	: Fourier transform infrared spectrometry
GC	: Gas chromatography
GC-FID	: Gas chromatography with a flame ionization detector
GC-MS	: Gas chromatography-mass spectrometry
H_2	: Hydrogen
HDO	: hydrodeoxygenation
HV	: Heat value
İ. D	: İnternal diameter

İRR	: İnternal rate of return
KBr	: Potassium bromide
Mo	: Molybdenum
MoO_3	: Molybdenum trioxide
MoP	: Molybdenum phosphide
MP	: Main product
N_2	: Nitrogen
NiMCF	: Nickel functionalized mesostructured foam silica
NİST	: National Institute of Standards and
NO_x	: Nıtrogen oxide
NPV	: Net present value
OA	: Oleic acid
Pd	: palladium
Pt	: Platinum
rpm	: revolution per minute
RTF	: Rich text format
SiO_2	: Silicon oxide
TGA	: Thermogravimetric analysis
TiO_2	: Titanium dioxide
TOFA	: Tall oil fatty acids
TPC	: Total plant cost
TPDC	: Total plant direct cost
TPİC	: Total plant indirect cost
TPR	: Temperature programmed reduction
ULSD	: Ultra-low Sulphur diesel
XRD	: X-ray powder diffraction
ZrO_2	: Zirconium dioxide

FIGURES LEGENDS

TABLES LEGENDS

1. INTRODUCTION

1.1. Background

The increasing energy requirement of emerging economies and the decline in fossil fuel reserves because of the over-exploitation have led to the development of new renewable energy sources. Energy depletion is a major concern for people today. This not only threatens the environment, but it has been a recurring issue for a long time due to various factors. One of these is the depletion of oil reserves. Despite the negative effects of fossil fuels on the environment, the demand for cleaner alternatives has remained high. The development of sustainable diesel fuels is expected to continue to be a promising trend (Abdulkareem-Alsultan et al., 2016).

One of the most effective ways to reduce greenhouse gas emissions is by using renewable energy sources such as biofuels. Unlike other energy sources, such as coal, biofuels are not only beneficial for the environment but are also used as a renewable source of energy (Gielen et al., 2019). These fuels can help to minimize oil dependency and also prevent the world from experiencing global warming. Despite the positive effects of biofuels, they should still not be regarded as the only solution to the world's energy problems. Aside from being beneficial for the environment, they also have to be used more sustainably to meet the goals of sustainability (Ikram et al., 2021).

The growing energy demand is an important factor that has contributed to global growth. The transportation sector is expected to be one of the most important factors contributing to global energy demand. Due to the movement toward more mobility in developing countries like Ethiopia, the demand for liquid fuels is expected to increase (Kebede et al., 2022). Several factors improve the prospects for renewable energy sources worldwide including rising oil prices, energy security, the environmental impact of fossil fuels, and strong government incentives.

1.2. Purpose of Study

This thesis aims to investıgatıon in the effect of different catalyst support of oleic acid on catalytıc deoxygenatıon to produce green diesel. The more specific objectives of the thesis are shown below.

- To characterize the prepared catalysts by using X-ray diffraction (XRD), Brunauer-Emmett-Teller (BET), Thermo-Gravimetric Analysis (TGA), and Scanning Electron Microscopy (SEM) analysis. This analysis is used to understand the coordination geometry of the catalyst and develop a structure-activity relationship;
- To characterize the deoxygenated liquid products by using Fourier-transform infrared spectroscopy (FTIR), Gas Chromatography-Mass Spectrometry (GC-MS), Higher heating value (HHV), and CHNOS analysis.
- To develop possible alternative processes using Superpro design for deoxygenation of non-edible oil as feedstock for the production of green diesel.
- An economic evaluation of various processes using appropriate models available in Superpro design.

1.3. Outline of Study

The thesis titled 'Investigation of The Effect of Catalyst Support of Oleic Acid on Catalytic Deoxygenation to Produce Green Diesel' illustrates the transition from CoMo-based catalysts to a different supported catalyst substance for deoxygenation reactions. The importance of this research work and the literature review that forms the background for this research work are detailed in sections 1 and 2.

The third section is about the experimental procedure. As its name says, what was done in the lab is explained step by step, following the order of the green diesel-making process. It starts with the preparation of different types of catalysts. Based on the performance of bimetallic catalyst systems, it was planned to develop CoMo based supported catalyst by impregnation method and evaluate its DO performance. Then, comes deoxygenated liquid product, where all the different methods that were tried are explained. Afterward is stated how the downstream separation of the products and how the cleaning was done. This is followed by an explanation of the different tests that were done to verify the quality of the deoxygenated liquid product.

Following the experimental procedure, there is a section that shows all the results obtained in the lab. The results of all the relevant experiments performed are presented. And then develop possible alternative processes using SuperPro design for deoxygenation of non-edible oil as feedstock for the production of green diesel with an economic evaluation of various processes using appropriate models available in SuperPro design. After that, a discussion of the results is done, stating their validity and key factors that help to understand the project. It is also discussed which are the best ways to produce green diesel and the advantages and disadvantages of deoxygenated liquid products. The last section is the conclusion and recommendations.

2. LITERATURE REVIEW

2.1. Introduction to Deoxygenation (DO) Process

The high fuel consumption and greenhouse gas emissions caused by the production of petroleum diesel are the main factors that motivate researchers to develop renewable energy sources. Producing green diesel from biomass, which can be derived from various sources such as animal fats, agricultural residue, and food processing equipment is a renewable energy source that can be globally available. Nowadays, green diesel is produced through various advanced technologies, such as hydrotreating, deoxygenation, and cracking reactions. Relative to petroleum, the obtained green diesel has a very low oxygen content and a high cetane number (Di Vito Nolfi et al., 2021).

The combustion of fossil fuels has been a vital part of the global energy supply since the industrial revolution. The rapid urbanization, industrialization, and increasing population have resulted in a significant increase in the demand for energy. Despite the various technological advancements that have occurred in the field of energy, Fossil fuels, including natural gas, petrol, and diesel, contributed almost 80% of the global primary energy consumption in 2019 (BP Energy, 2019). However, it's believed that the oil and gas reserves will run out in around ~50 years (Ritchie, Hannah; Roser, 2018).

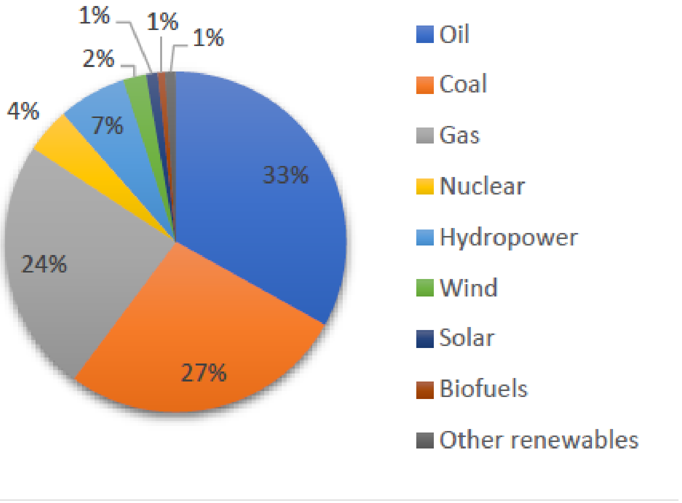

Source: BP Energy (2019)

Figure 2.1. Global primary energy consumption

Vegetable oil, animal fat, and waste oils are highly utilized to supply biodiesel (Da Mota et al., 2014). However, the presence of a high number of oxygen-bonded molecules in biodiesel lead to oxidative instability, which lowers the preservation stability. Also, this yields to inadequate quality of flow properties and subsequently limits high-grade fuel's direct application. Therefore, various processes have been developed to improve the quality of renewable diesel by producing it in compliance with the latest infrastructure. Cracking and deoxygenation pathways are promising methods to overcome this problem.

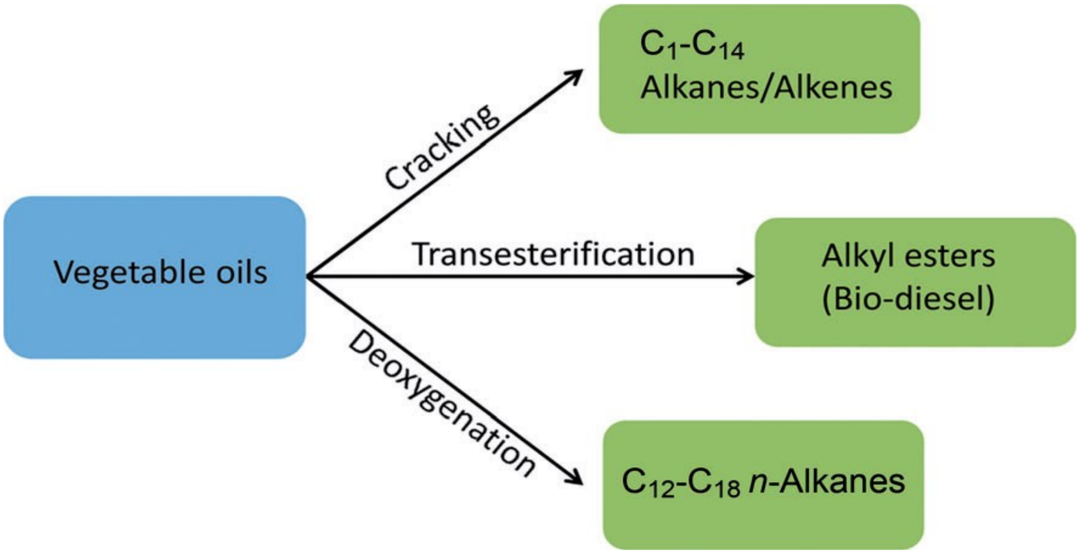

Source: https://chemistry-europe.onlinelibrary.wiley.com/doi/10.1002/cssc.201300370

Figure 2.2. Vegetable oil upgrading processes

Cracking is the thermochemical or catalytic decomposition of triglycerides. The main products are lighter alkanes, alkenes, and fatty acids. Conventional cracking catalysts used in the petrochemical industry, that is, zeolites and mesoporous aluminosilicate, can also be applied to vegetable oils. The process is, however, highly unselective as a large range of hydrocarbons and oxygenates are formed (Yeletsky et al., 2020). Therefore, cracking is not the optimal upgrading technology of vegetable oils for the production of diesel-type biofuels.

Transesterification is currently the major process that is commercially applied to produce biodiesel from vegetable oils. The resulting fatty acid methyl esters (FAMEs) not fully compatible with conventional diesel engines owing to the still relatively high oxygen content of fatty acid esters. As a result, this type of biodiesel must be blended with petroleum fuel, or engines must be adapted. Other disadvantages of FAMEs are the poor cold-flow properties because of the high cloud point, pour point, and cold filter plugging point. In addition, the abundant use of homogeneous base catalysts and the high downstream processing costs further restrain this upgrading technology (Gaurav et al., 2019).

Aside from bulk chemicals, vegetable oils can also be used to produce higher value chemicals, such as those that are used in the production of linear alpha-olefins. This process can be done through the tuning of catalytic deoxygenation to produce higher value chemicals. One of the most important factors that has attracted this interest is the development of a process that can decarboxylate unsaturated fatty acids using a combination of catalysts (Rashidi et al., 2022).

The deoxygenation of oleic acid is carried out through two major reaction pathways. These pathways allow the production of green diesel (Hermida et al., 2015);

(i) the decarbonylation (DCO) pathway involves the removal of carbonyl groups through C-C and C-O bond cleavage to provide straight-chain alkenes releasing carbon monoxide and water as by-products and

(ii) (ii) decarboxylation (DCO_2), which involves the removal of carboxyl groups by the cleavage of the C-C bond and also the release of carbon dioxide to provide a straight-chain alkane with one atom.

Due to the increasing number of studies on the various aspects of solid acid catalysts, such as their performance in the deoxygenation reaction, researchers have started to focus on the use of noble metal-based catalysts. These are known to exhibit high performance and produce a high yield of various hydrocarbon components of solid acid catalysts involving metal sulfides, metal phosphides, metal carbides, noble metals, (Hsu and Lin, 2017; Janampelli and Darbha, 2018), and d-block metal oxides upheld on various oxide materials (e.g., CeO_2, TiO_2, and SiO_2). Also, noble metal-based catalysts are reported to exhibit great catalytic performance in deoxygenation reactions (M. Liu et al., 2020). Although the high prices of metal-based catalysts prevent their use in the industry, they are still considered promising materials for the deoxygenation reaction. In recent studies, researchers have shown that the use of basic metal catalysts can improve the performance of the process (Afshar Taromi and Kaliaguine, 2018).

In an inert environment, Mo oxide-supported γ-Al_2O_3 catalysts were able to deoxygenate a wide range of unsaturated fatty acid compounds, such as oleic acid and monounsaturated fatty acid. The performance of the process was achieved with 80% selectivity for C_{17} compounds. Mo oxide-based catalysts have been widely used in the hydrodeoxygenation of petroleum products. (H. Wang et al., 2019). Studies supporting the use of Co-Mo species in the hydrodeoxygenation process have revealed that the acid-base characteristics of the compounds can be improved by incorporating Mo and Co species. According to Mora-Vergara et al., the formation of giant acidic sites on CoMo promoters was due to the synergism between the two metals (Mora-Vergara et al., 2018).

The catalyst support is a vital component of the process of deoxygenation that helps promote the diffusion of active metals and increase the active sites. Active carbon is known to have a high extent of activation and a low propensity toward coke formation. AC is also thermally stable, which limits the sintering of dynamic metals during the deoxygenation response. Co-supported by carbon has also been studied in the reaction, but the resulting green diesel was composed of unsaturated species The catalyst was developed with a sulfur-free composition. It was then deoxygenated oleic acid and produced a saturated green diesel. The reaction was performed with various supporting compounds, such as CeO_2, Zeolite, and TiO_2 (Asikin-Mijan et al., 2017).

2.2. A Comparison of Fuel Properties: Green Diesel vs. Other Diesel

Compared to conventional diesel oil, which is produced from petroleum products, green diesel is eco-friendly and more economical to use. It is derived from plants and animal fats and doesn't contain harmful emissions. Green diesel is created from animal facts and plants and According to a study conducted by Di Vito Nolfi indicated that green diesel is a type of second-generation diesel that's derived from various renewable resources such as biomass, thermal, and hydrotreating. This fuel is chemically similar to regular diesel (Di Vito Nolfi et al., 2021). Biodiesel is a type of fuel that's produced by combining alcohol and esters by transesterification reactions.

Table 2.1. The typical properties of Petro diesel, biodiesel, and green diesel

Properties	Petrodiesel	Biodiesel	Renewable Diesel (Green Diesel)
Cetane#	40-45	50-60	75-90
Energy Density, MJ/kg	43	38	44
Density, g/ml	0.83-0.85	0.88	0.78
Energy Cont., BTU/gal	129 K	118 K	123 K
Cloud point, °C	-5	20	-10
Oxidative stability	Baseline	Poor	Excellent
Clod flow Properties	Baseline	Poor	Excellent
Lubricity	Baseline	Excellent	Baseline
Sulfur	<10 ppm	<5 ppm	<10 ppm
NO_x Emissions	Baseline	+10	-10 to 0

Source: (Yoon, 2009)

2.3. Alternative Pathways for the Production of Green Diesel

2.3.1. Deoxygenation

Biofuels are usually produced through chemical reactions in the absence of oxygen known as deoxygenation. However, due to the high levels of oxygen in the air, this process can negatively affect the quality of the finished product. This is why the process must be carried out properly. The decarboxylation/decarbonylation process that removes the oxygenated compounds in the form of CO_2/CO through direct C–O bond cleavage under H_2-free conditions and produces hydrocarbons., a process known as deoxygenation. This method is commonly used by researchers to alter the composition of the finished product (Anwar et al., 2021). Catalytic deoxygenation is carried out through a chemical reaction that's designed to improve the quality of the finished product. This process can be used to increase the production of hydrocarbons-based fuels. According to the researchers, indicated that catalytic deoxygenation can be specifically used to optimize the composition of the biofuel product. In catalytic deoxygenation, hydrodeoxygenation is used to successfully eliminate the atoms from the triglycerides. In the chemical process, HDO is commonly used to overcome the hydrogen problems caused by deoxygenation. In the initial step, deoxygenation can be used to reduce the coke deposition (Rogers and Zheng, 2016).

A study conducted by Mijan revealed that the use of curcas oil can be used to produce green fuel, which is considered to be a sustainable alternative to petroleum products. It could reduce the greenhouse gas emissions associated with the production of green diesel. The reduction of greenhouse gas emissions by the use of green diesel has greatly improved the transportation and industrial sectors. According to researchers, the process used to extract green diesel from any source of oil without using oxygen is known as deoxygenation. A multi-walled carbon nanotube is also used to improve the quality of the oil. The researchers noted that the use of Ni-Co in the deoxygenation process leads to higher levels of activation in the oxidization sites. It also produced a higher unsaturated and saturated hydrocarbon content (Asikin-Mijan, Lee, Juan, et al., 2016).

2.3.2. Hydrodeoxygenation (HDO)

In the production of green diesel, hydrodeoxygenation is carried out. This process removes the oxygen from the biomass by producing various compounds, such as fatty acids and triglycerides. These are then used to form the n-paraffins and water. Through hydrodeoxygenation, bio-oils are then upgraded through a process that is considered promising for the production of liquid transportation fuels. The quality of the bio-oils and the catalysts used during the process are some of the factors that are considered when it comes to the smooth transition of renewable fuels into liquid transportation fuels (Krobkrong et al., 2018).

The composition of bio-oils and their upgradations through hydrodeoxygenation were discussed by the researchers. In this study, the researchers discussed the various routes that model compounds can adopt when it comes to the development of new products using different catalysts. They also discussed the various steps involved in the reaction of different compounds through the HDO process. Some of these include the hydrotreating of sulfides, phosphides, and non-metals such as bio-metallics and reduced bronzes (Alsultan et al., 2017).

2.3.3. Pyrolysis

When there is not enough oxygen available to properly heat the organic materials, such as biomass, pyrolysis is used. This process breaks down the chemical composition of the materials into gases and charcoal. The presence of oxygen is required to properly conduct combustion, but the chemical composition can also be easily decomposed. Pyrolysis is mainly used to heat the organic materials, such as biomass When the different volatile gases are converted into a liquid, this process can facilitate the healing of the biomass. This process can also be used to produce various products, such as bio-oil, bio-char, and syngas (Safa Gamal et al., 2019).

Besides being used to heat the organic materials, this process can also be used to produce various other chemicals. When the temperature reaches 500 °C, the various factors that affect the production of bio-oil become equal, and the heating rate reaches around 1000 °C/s. This process is known as fast pyrolysis. During this process, a large amount of bio-oil is produced by heating the biomass feedstock, which is composed of 65% bio-oil, 25% biochar, and 10% syngas. Slower-burning processes are referred to as bio-char processes, which are characterized by the production of biochar instead of bio-oil. These are usually self-sustained since they are carried out using a combination of biomass and syngas combustion provides the required energy to drive the reaction as shown in the figure below.

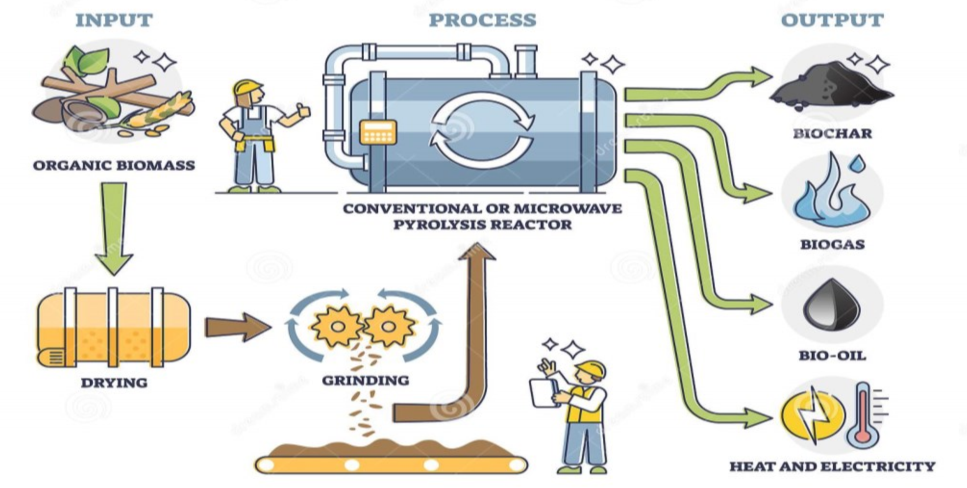

Source: https://image.shutterstock.com/image-vector/biochar-biogas-bio-oil-energy-600w-2053877978.jpgs

Figure 2.3. Pyrolysis heating process to produce bio-oil, bio-char, and syngas

2.4. Feedstocks for Deoxygenation Process

A wide variety of vegetable oils are ideal for the production of diesel fuel due to their chemical structure. Usually, plant oils are composed of various types of fats, such as those that are free fatty acids, diglycerides, and triglycerides. However, due to the varying crop growing patterns in different regions, the choice of feedstock can be determined. Aside from the geographical location, factors such as the availability of raw materials and the environmental impact of the production process should also be considered when choosing a potential feedstock for the reaction. Bio-based fuels have a lot of advantages over conventional fuels. These include their ability to reduce greenhouse gas emissions and their stable supply of raw materials (Jain et al., 2016).

Various studies have been conducted on the deoxygenation reactions of various compounds. One of the most common types of vegetable oils is oleic acid, which is the primary component of both green seed oil and canola oil. Linolenic acid and linoleic acid are also abundant fatty acids. Linolenic acid and oleic acid are also carboxylic acids, which are composed of C_{18} atoms. Their hydrogenation and hydrodeoxygenation are the key steps in the production of diesel fuel from green seed oil or canola oil.

2.5. Choice of Support for Deoxygenation Process

One of the most important factors that can affect the deoxygenation activity of a given catalyst is the choice of support. For instance, the use of γ-Al_2O_3 supports is commonly used for various catalysts (Z. Zhang et al., 2016). However, this support can also cause catalyst deactivation due to the formation of coke. To minimize the effects of the support on the catalyst's deoxygenation activity, various alternative materials such as TiO_2, SiO_2, ZrO_2, zeolites, and various metal oxides were used in the preparation of dopants. One interesting fact about these materials is that their support can be tailored depending on the method used (H. Zhang et al., 2021).

Ooi et al. 2019 studied the deoxygenation of rapeseed oil by using various support materials, such as SiO_2, Al_2O_3, and nickel. It was observed that the product selectivity of these supports was affected by their nature. The study revealed that the CoMo catalyst supported by titanium dioxide exhibited low selectivity for the deoxygenation of rapeseed oil. In addition, the active phase was not well distributed.

2.6. Proposed Reaction Scheme For Catalytic Deoxygenation

The product distribution of a deoxygenated liquid product is shown in Figure 2.4. The results of a GC-MS analysis revealed that the various supported catalysts exhibited higher n-(C_8–C_{20}) hydrocarbon distribution (>80%), which suggests that they are promising for promoting the deoxygenation activity and converting oleic acid into green diesel. The oleic acids are then deoxygenated through decarboxylation. These compounds are then converted into saturated n-heptadecanes ($C_{17}H_{36}$) and mono-unsaturated n-heptadecanes ($C_{17}H_{34}$). In this process also yields gaseous CO_2 as a byproduct. Meanwhile, the oleic acid undergoes a decarbonylation reaction by the removal of CO and H_2O as byproducts, thereby producing hydrocarbons with extra double bonds in the form of di-unsaturated ($C_{17}H_{32}$), mono-unsaturated ($C_{15}H_{30}$, $C_{17}H_{34}$), and poly-unsaturated ($C_{17}H_{28}$) compound.

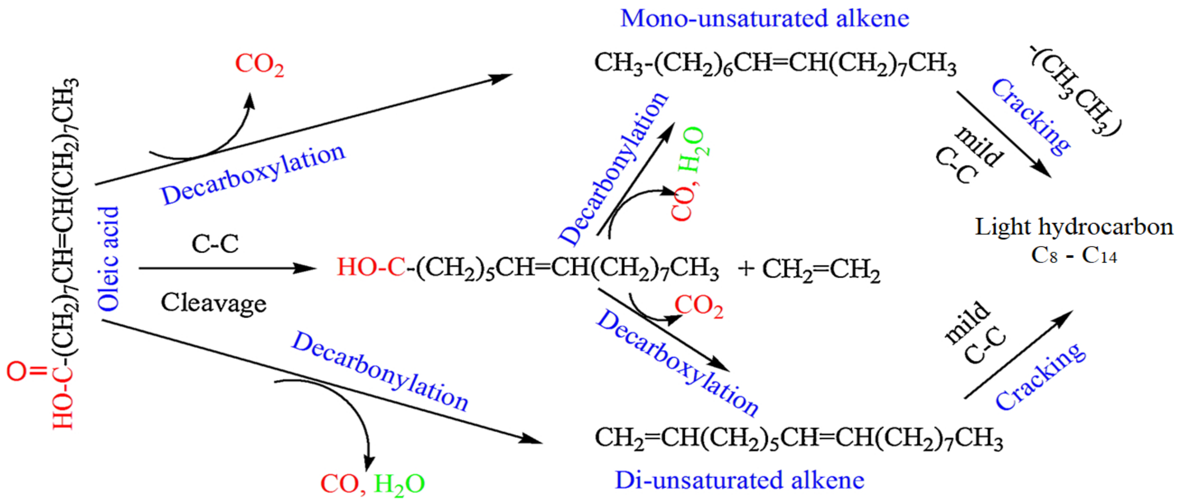

Figure 2.4. Proposed reaction pathway for catalytic deoxygenation of oleic acid

Furthermore, the cracking of liquid products that have been deoxygenated may also lead to the formation of n-C_{15} compounds, similar to what happened when cooking oil was deoxygenated using a nanorod-activated carbon. This phenomenon is consistent with Kareem's previous work, which showed that the use of a walnut shell's nanorod-activated carbon enabled the production of n-C_{15} from waste cooking oil (Alsultan et al., 2017).

2.7. Factors Influencing The Deoxygenation Process

Accomplishing the high content of diesel-like hydrocarbons in liquid products are important in the deoxygenation of fatty acid and triglycertor to avoid further separation step such as distillation to meet a quality standard as a fuel (Sari et al., 2013). The conditions that affect the yield and selectivity of certain types of fuels are known to have a significant influence on the product composition and quality of the diesel-like hydrocarbon. Several process conditions are reported in the literature, such as the temperature, feed type, reaction atmosphere, and catalyst loading. Although the exact effects of these conditions are yet to be studied, it is believed that they have a significant influence on the overall performance of the process.

2.7.1. Supported Metal Catalyst Type

Various supported metal catalysts, such as Ni, Pd, and Pt, have been studied for the deoxygenation of waste fat by hydrogenation. It has been observed that the Ni, Pd, and Pt catalysts are more active than the Pt/γ-Al_2O_3 catalysts when it comes to producing C_{17} and C_{15} diesel hydrocarbons. The higher activity of the Pd/γ-Al_2O_3 catalyst was due to the presence of a more active metal. However, despite having the highest active metal, the Ni catalyst showed the lowest activity when it comes to producing diesel-like hydrocarbons. This result was attributed to the large particle size of Ni in the Ni/Al_2O_3 catalyst was the reason why it exhibited the lowest activity. In terms of particle size, the average size of Ni in the catalyst was 8.2 nm, while that of Pd and Pt was 4.6 and 5.4 nm.

Meanwhile, Nickel (Ni/C) is a more selective and active catalyst for the deoxygenation of diesel-like hydrocarbons using mesoporous carbon compared to Pt or Pd. This advantage was due to the higher content of Ni in the Ni/C catalyst. Furthermore, in various Ni functionalized mesostructured cellular foam silica (NiMCF) the nickel content of the catalyst was found to be higher than that of Pd or Pt. It was also the most active catalyst for the deoxygenation of palmitic acid using solvent less. The metal particles were also active sites for the production of alkene and n-alkane fatty acid deoxygenation through decarboxylation and decarbonization reactions, respectively (Roh et al., 2011). It can be concluded that metal-based mesoporous materials are suitable for the production of diesel-like hydrocarbons by deoxygenation.

2.7.2. Amount of Catalyst

Catalysts are critical to optimize the product distribution and selectivity for desired products. Catalyst characteristics, such as pore structure and pore volume with area have significant effects on deoxygenation reaction property and product selectivity. The amount of catalyst used for deoxygenation effect’s reaction rates and selectivity to certain products, such as heptadecane and n-heptadecane. A study has been conducted on the effects of catalyst amount on the conversion and reaction rates of stearic acid in dodecane. The results indicated that the higher the catalyst in the range, the more conversion and reaction rates would increase. However, the increase in the catalyst amount has a negative effect on the activation of the n-heptadecane and the reduction in the catalyst's selectivity. This is a critical parameter that can be used in optimizing the yield of the products. Tran et al. (2021) reported that, increase in the amounts of NiMo/Al_2O_3 catalyst (0 – 0.126 g) significantly decreased the methyl laurate deoxygenation at 350 °C (Q. K. Tran et al., 2021). The researchers also found that the increase in the catalyst amount led to a decrease in the selectivity and conversion of linear hydrocarbons into dodecane and undecane. This resulted in the formation of various undesirable products.

2.7.3. Feed Types

In recent years, the focus has been on the use of biomass-based feedstocks in the production of renewable energy. The majority of biomass-derived substrates are composed of carbohydrates. These are then converted into renewable energy using a combination of platform molecules (Reid et al., 2020). Due to their sustainable nature, these materials have gained interest in the production of energy. However, the process of converting these biomass-based molecules into chemicals is encountering various challenges due to the high oxygen content in the saccharides (Z.-H. Liu et al., 2021).

A study conducted on polyols revealed that they are ideal candidates for the production of chemicals and renewable fuels from biomass. The researcher also noted that the hydrogenation of the biomass has poor solubility due to the presence of organic solvents. The research conducted by Pattanaik and Misra shown that efficient deoxygenation reactions are essential to derivate sugar and cellulose in the presence of high temperature and acid-catalyzed dehydration (Pattanaik and Misra, 2017).

The large quantities of unsaturated compounds decreased the n-alkane selectivity. At a 30 % deoxygenation, the stearic acid methyl ester gave an n-alkane selectivity of 40%, which is lower than that of the stearic acid (Gosselink et al., 2013). On the other hand, the deoxygenation of the behenic acid resulted in an n-alkane selectivity of 80%, which is higher than that of the fatty acid. This suggests that the decarboxylation reaction is more dominant in the oxidation of behenic acid. This was due to the easier breaking of the COO– H bond in fatty acid compared to the COO–R bond in fatty acid ester, because the alkyl group in ester is a nucleophilic group as reported in the literature (Hermida et al., 2015).

The higher n-alkane selectivity of the behenic acid was due to the easier breaking of the COO-H bond in fatty acid compared to in fatty acid. It was also reported that the deoxygenation of stearic acid produced CO as the main gaseous compound. The results of the study revealed that the deoxygenation of fatty acid resulted in a higher n-alkane selectivity, as compared to that of stearic acid. This suggests that the decarboxylation reaction is more dominant in the oxidation of behenic acid (Fangkoch et al., 2020). The higher n-alkane selectivity of saturated fatty acid was also achieved by deoxygenation with a shorter chain. In addition, the deoxygenation of palmitic acid was performed using a mesoporous carbon catalyst in the presence of dodecane as solvent in a semi-batch reactor at 300 °C under 5 % H_2 in argon (Lestari et al., 2009).

The reaction rate of palmitic acid with stearic acid was found to be the same as that of stearic acid. This result supports the findings of other researchers who reported the same reaction rate for various deoxygenations, such as stearic acid, behenic acid, behenic acid, nonadecanoic acid, and heptadecanoic acid (Simakova et al., 2010). The resulting products, namely n-pentadecane and n-heptadecane, are the main liquid products.

2.7.4. Reaction Temperature

According to the researchers, the temperature difference between 300 °C and 360 °C resulted significantly affected the deoxygenation of dodecanoic acid in a reactor in the increase in conversion from 10 % to 60 % with undecane and undecane as the main products (Bernas et al., 2010). For deoxygenation of stearic acid in a semi-batch reactor, the temperature increases from 270 °C to 330 °C significantly reducing the time needed for conversion from around 270 °C to 20 minutes. The increase in temperature also resulted in an increase in the conversion rate of ethyl stearate from 40 to 100 percent. On the other hand, the selectivity of n-heptadecane decreased from 70 to 40 percent. The deoxygenation was carried out in a semi-batch reactor with the flow of 5 % H_2 in argon. The temperature at which the deoxygenation of TOFA takes place has been studied (Mäki-Arvela et al., 2007).

It was found that the temperature difference between 300 °C and 350 °C can affect the performance of the dodecane solvent. The total conversion of fatty acid increased with the increase in the reaction temperature. However, minor interring of the Pd/C occurred only at a reaction temperature of 350 °C (Kwon et al., 2011). The main products in this liquid phase, namely n-heptadecene and n-heptadecane, were preferred products when the temperature reaction was 300 °C.

2.7.5. Reaction Atmosphere

The research work conducted by Pattanaik and Misra investigated the effects of the reaction environment on the deoxygenation process of bio-oils. They found that the reaction atmosphere can affect the efficiency of the process. Fossil fuels have become more prevalent due to their environmental protection. According to the research, The discovery of the second generation of liquid hydrocarbon fuels, which can be produced through the deoxygenation of vegetable oils and fatty acids, attracted the attention of various renewable energy developers (N. T. T. Tran et al., 2016). However, the researchers noted that the fuel's higher oxygen content could pose a threat to the operation of diesel engines. Therefore, the researchers investigated that reaction temperature, reaction atmosphere, and feed type can make a considerable factor influencing the operating parameters of the catalysts used in the production processes of catalytic deoxygenation.

3. MATERIALS AND METHODS

3.1. Materials

Cobalt (II) nitrate hexahydrate (Co $(NO_3)_2.6H_2O$) and ammonium heptamolybdate tetrahydrate ($(NH_4)_6Mo_7O_{24}.4H_2O$) which has a purity of 98.5% was purchased from Sigma Aldrich (UK), Titanium dioxide (TiO_2) with the purity of 99.0% was provided by Evonik Industries, Aluminum oxide (γ-Al_2O_3) and oleic acid (> 99%, Sigma-Aldrich). The N_2 gas has a purity of 99.0% and GC solvent n-hexane grade (98.5%, Anidrol).

3.2. Catalyst Preparation

The introduction of CoMo onto the CeO_2 support was carried out by the incipient wetness impregnation method, using cobalt nitrate hexahydrate (Co $(NO_3)_2\cdot 6H_2O$) as the precursor.

✓ The Amount of Cobalt and Molybdenum required (Co_xMo_y/ CeO_2), x = y

✓ $\frac{X}{X+y\ +0{,}5\ g\ of\ \text{CeO2}} = \frac{5}{100} \rightarrow \frac{X}{2X\ +0{,}5\ g\ of\ \text{CeO2}} \rightarrow X = 0{,}0278\ g\ of$ Cobalt

✓ From the stoke

$$\text{Co} = 0.0278\ g * \frac{1\ mol\ Co}{58{,}93\ g\ Co} * \frac{1\ mol\ CNHH}{1\ mol\ Co} * \frac{291.04\ g\ CNHH}{1\ mol\ CNHH} * \frac{100}{99{,}3}$$

$$= 0.14\ g\ of\ Co\ from\ \text{CNHH}$$

Similarly, for Mo

$$\text{Mo} = 0.0278\ g * \frac{1\ mol\ Mo}{95.95\ g\ Mo} * \frac{1\ mol\ AMTH}{7\ mol\ Mo} * \frac{1235.9\ g\ AMTH}{1\ mol\ CNHH} * \frac{100}{99{,}3}$$

$$= 0.05\ g\ of\ Mo\ from\ \text{AMTH}$$

Prepare a solution of 0,14 g of Cobalt and 0.05 g of Molybdenum in 100 ml of distilled water and similarly 0,5 g of CeO_2 in 25 ml of distilled water and mixed continuously at temperature of 50 °C for approximately 6 h with 280 rpm. After mixing for 6 hr and then the sample was dried at 110 °C for another 12 hrs. The dried sample was decomposed by thermal calcination at 550 °C for 4 hrs. under static air. Before proced to the reaction step, these samples need to be reduced by the flowing hydrogen. The reduced catalysts are referred to as CoMo/CeO_2. The AC, γ-Al_2O_3, TiO_2, and Zeolite support of the CoMo was prepared with a similar preparation method, and catalysts denoted as Co_5Mo_5/AC, Co_5Mo_5/Al_2O_3, Co_5Mo_5/TiO_2, and Co_5Mo_5/ zeolite.

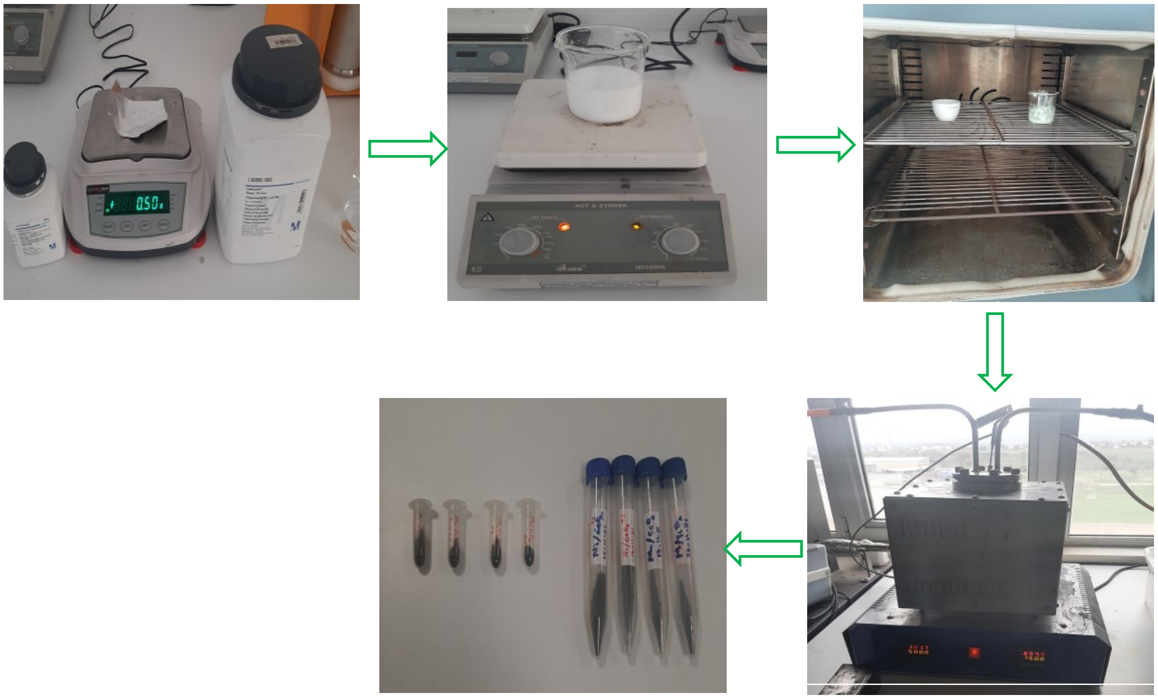

Measuring the required chemicals

Magnetic Stirring (280 rpm) at a temperature of 50 °C

Drying the samples

Making a calcination

Sample preparation for analysis

Figure 3.1. Preparation of catalyst

3.3. Catalyst Characterization

Brumaire-Emmett-Teller (BET) technique is the method that used an N_2 adsorption/desorption analyzer (Thermo-Finnigan Sorpmatic 1990 series). it had been employed to assemble knowledge into the extent and therefore the features of the catalysts' pore size and volume distribution.

The X-ray diffractometer instrument of Shimadzu, the XRD-6000, was used to study the dispersion states of various catalysts.

The catalyst surface morphology and determining the Co, Mo, C, O, Al, and Ce elemental composition of the catalysts were analyzed by scanning electron microscope (SEM).

Thermogravimetric analysis was applied to gauge the thermo-stability of the synthesized catalyst using (TGA, Mettler Toledo 990). The catalyst was heated under a 50 mL/min N_2 stream gradually to 900 °C at a rate of 30 °C/min.

3.4. Catalytic Deoxygenation of Oleic Acid

The catalytic deoxygenation of oleic acid was carried out in a 250 mL semi-batch reactor with mechanical stirring, containing 25 mL of oleic acid and 5 wt% catalysts (Figure 3.2). Before the heating process, the reactor was cleaned with nitrogen gas to discharge the oxygen gas. The reactor temperature gradually increased to 350 °C with constant stirring (300 rpm) and was held for 60 min under 20 mL/min of N_2 gas flow rate. A blank test, in the absence of the catalyst, was carried out, with the objective of evaluating the importance of catalyst of thermal deoxygenation at 350 °C. The vapor produced was condensed by the cold water (20 °C) and collected in a receiving tank. On completion of the reaction, the reactor was left to cool down to room temperature. The deoxygenated liquid product was weighed and analyzed by gas chromatography-mass spectrometry (GC-MS), Fourier transform infrared spectrometry (FTIR), Oxygen Bomb Calorimeter tests, Elemental analysis for carbon, hydrogen, nitrogen, oxygen, and sulfur (CHNO-S). All the experimental reactions were repeated three times and the results were evaluated as the average of the three repetitions.

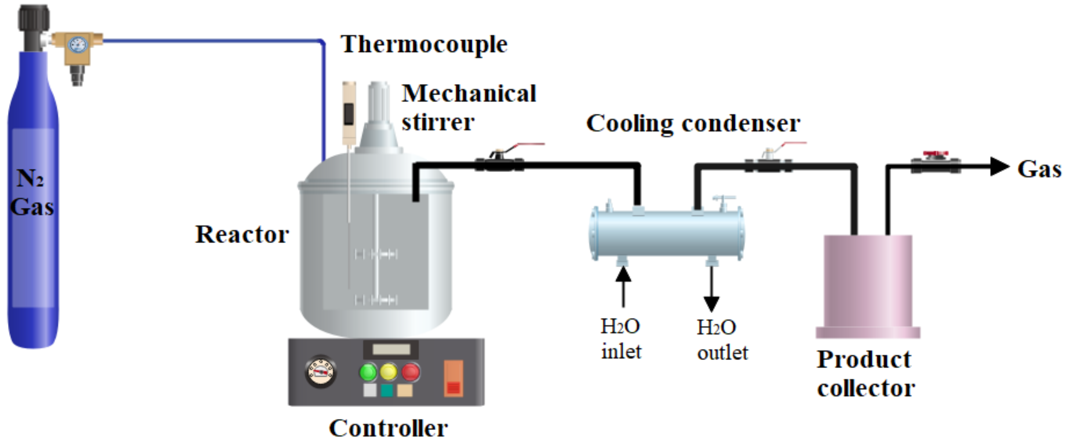

Figure 3.2. The schematic diagram for catalytic DO reaction.

Oleic acid conversion had been calculated

$$\text{Oleic acid conversion (\%)} = \frac{n_{OA,in} - n_{OA,out}}{n_{OA,in}} x\ 100 \qquad \textbf{(3.1)}$$

3.5. Product Analysis

The Fourier-transform infrared spectroscopy (FTIR) was performed at room temperature on a Nicolet 6700 spectrometer with a resolution of 4 cm $^{-1}$ and a wavelength range of 4000 cm $^{-1}$ to 400 cm $^{-1}$. This analysis was used to identify the functional groups present in oleic acid and the liquid products. To prepare the samples, 1 mL of KBr was dropped on 1 g of the sample followed by heating at 150 °C overnight. Then, pellets were made mixing 200 mg of KBr and 1 mg of sample.

The product distribution of the monounsaturated fatty acid and deoxygenated liquid products were characterized qualitatively using GC-MS (Shimadzu model QP5050A) equipment with a non-polar HP-5MS column (30 m × 0.25 mm × I. D µm) with a split-free inlet. The Samples were diluted with >98% purity GC grade n-hexane. The results of the study were further analyzed using the NIST library. The objective of the study was to enhance the understanding of the component peaks of the GC-MS spectrum. The key products (such as hydrocarbon fractions, carboxylic acids, ketones, alcohols, and cyclic compounds) that were identified by the instruments were compared with the probability matches between 95% and 100%.

The CAL3K-U model oxygen bomb calorimeter is the most widely used method to obtain the enthalpy of the formation of solid and liquid organic compounds. The most common application is determining the calorie content of feces or a special diet. The ignition and combustion process takes place in a chamber called a 'bayonet bomb', so the energy released can be measured as heat. Benzoic acid is used as standard calibration of an oxygen bomb calorimeter system to ignite the sample. The container is filled with oxygen at the oxygen filling station after which the prepared container is placed in the calorimeter. Once run, the vessel is placed in the air cooler for 8 minutes to cool down again and prepare for the next sample.

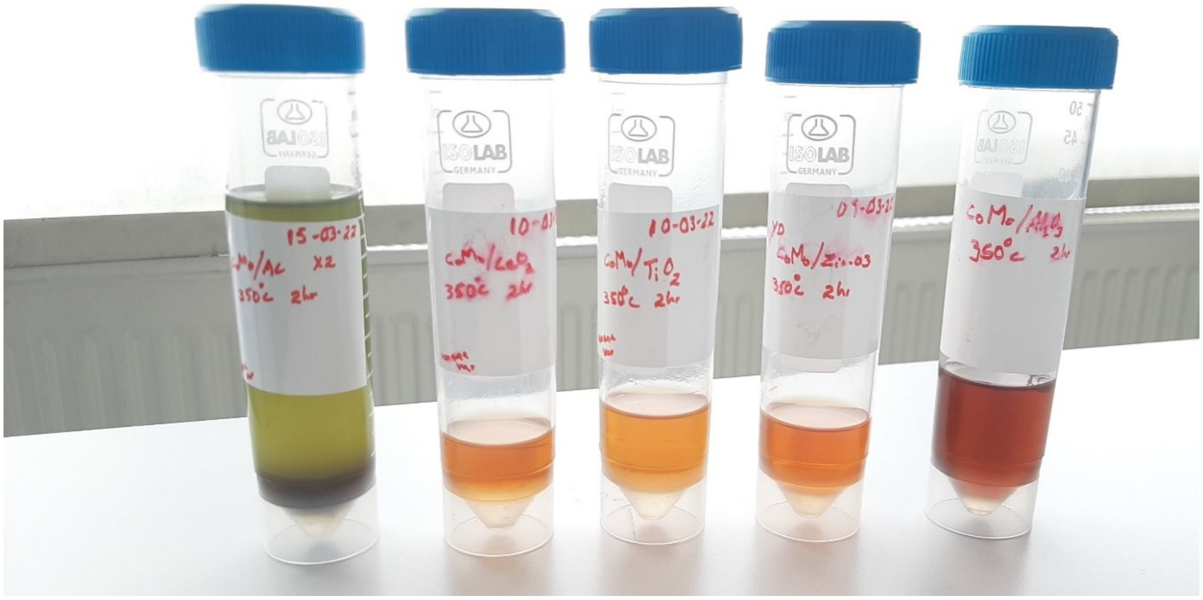

Figure 3.3. Green diesel product obtained from oleic acid deoxygenation reaction using catalyst

4. RESULT AND DISCUSSION

4.1. Catalyst Characterization

4.1.1. XRD Analysis

The XRD patterns of various CoMo/AC, CoMo/Al_2O_3, and CoMo/Zeolite catalysts are shown below. The reduction in the AC matrix's overall amorphous texture was caused by the intercalation of the Mo and Co species. The XRD characteristics for the bimetallic catalyst CoMo peaks representing in the cerium oxide are clearly shown at 2θ = 28.62°, 33.58°, 47.58°, 56.37°, 59.16°, 70.01°, 77.04°, 79.41°, and 88.48°. This show that the high-intense CeO_2 peak indicates that CoMo is not fully dispersed on the support surface. In the case of CoMo/AC and CoMo/Zeolite, both catalysts showed that the less-intense CoMo peak shows that fully dispersed on the support surface of active carbon and zeolite. The XRD characteristics for titanium oxide the peaks appeared at 2θ = 25.01°, 39.33°, 48.37°, 54.38°, 55.71°, 62.15°, and 76.41. The presence of aluminum oxide species has led to the formation of a cubic structure consisting of 2θ = 25.52°, 26.18°, 35.15°, 51.92°, 56.37°, 57.51°, 66.25°, 67.48°, and 77.94°. The high-intense γ-Al_2O_3 peak shows that CoMo is not fully dispersed on the support surface.

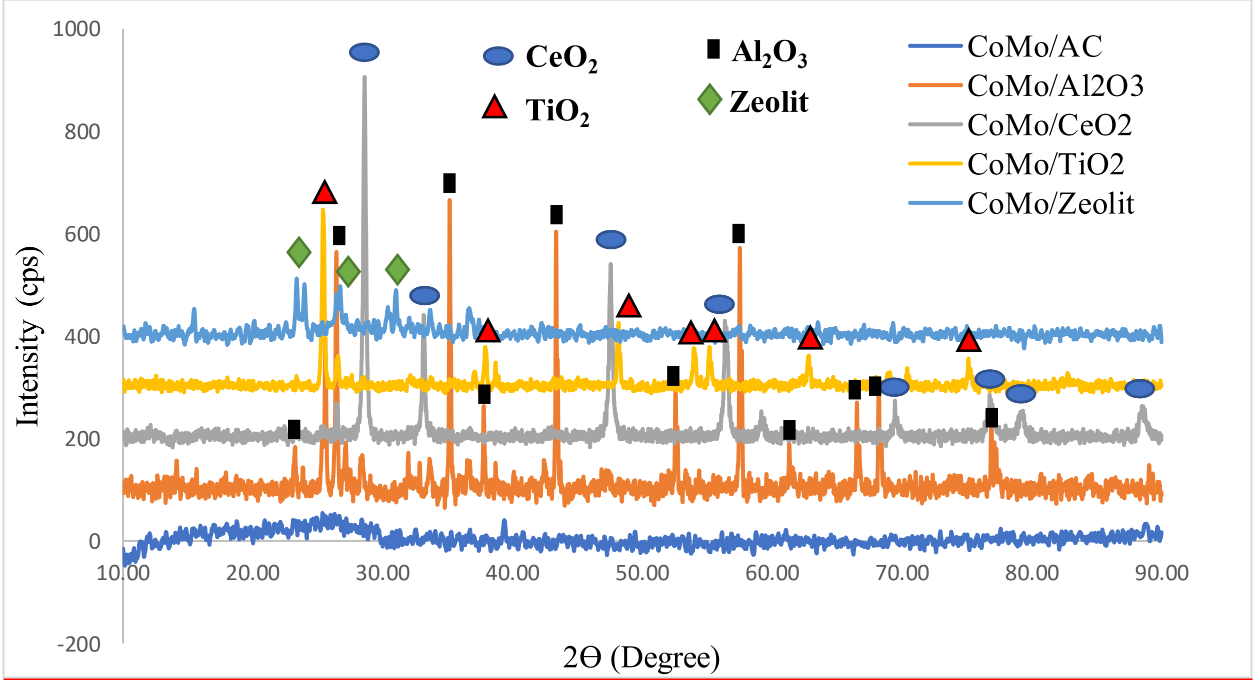

Figure 4.1. XRD patterns of CoMo/AC, CoMo/Al_2O_3, CoMo/CeO_2, CoMo/TiO_2, and CoMo/Zeolite catalyst

4.1.2. BET Surface Area Analysis

The pore volume and surface area of all synthesized catalysts were determined using the BJH and BET methods. The results in Table 4.1 below indicated that the various support materials exhibited higher surface area, such as AC (317.37 m^2/g), Al_2O_3 (12.30 m^2/g), and Zeolit (92.75 m^2/g). It was also perceived that the surface area of these materials was reduced after they were incorporated with the CoMo, the pore volume decreased gradually. The reduction in the surface area of the pore due to the presence of excessive amounts of active metals was most likely caused by the buildup of these materials in the pores (F. Wang, Jiang, et al., 2018). Rather, the enlarged pore diameter was caused by the downfall of the walls during the process of impregnation and partial destruction after calcination. The larger pores are commonly used to disperse the resulting materials on a catalyst, and they can also stimulate the deoxygenation process.

Table 4.1. Physicochemical property of the synthesized catalysts.

Catalyst	N_2 adsorption-desorption analysis		
	Surface area (m^2/g)[a]	Pore volume (cm^3/g)[b]	Pore diameter (nm)[b]
CoMo/AC	317.37	0.465	5.654
CoMo/Al_2O_3	12.30	0.025	5.729
CoMo/CeO_2	16.95	0.053	7.675
CoMo/TiO_2	7.54	0.056	19.330
CoMo/Zeolite	92.75	0.138	8.751

[a] Determined from BET analysis.

[b] Determined from BJH analysis.

4.1.3. Thermo-Gravimetric Analysis (TGA)

Thermo-gravimetric analysis (TGA) was employed to study the thermal stability of the synthesized catalysts. The results of the study, which were presented in Figure 4.2, showed that the various metal catalysts exhibited no significant mass loss when they were placed in the temperature range of 25–350 °C. This indicates that they were able to maintain their thermal properties in this temperature range.

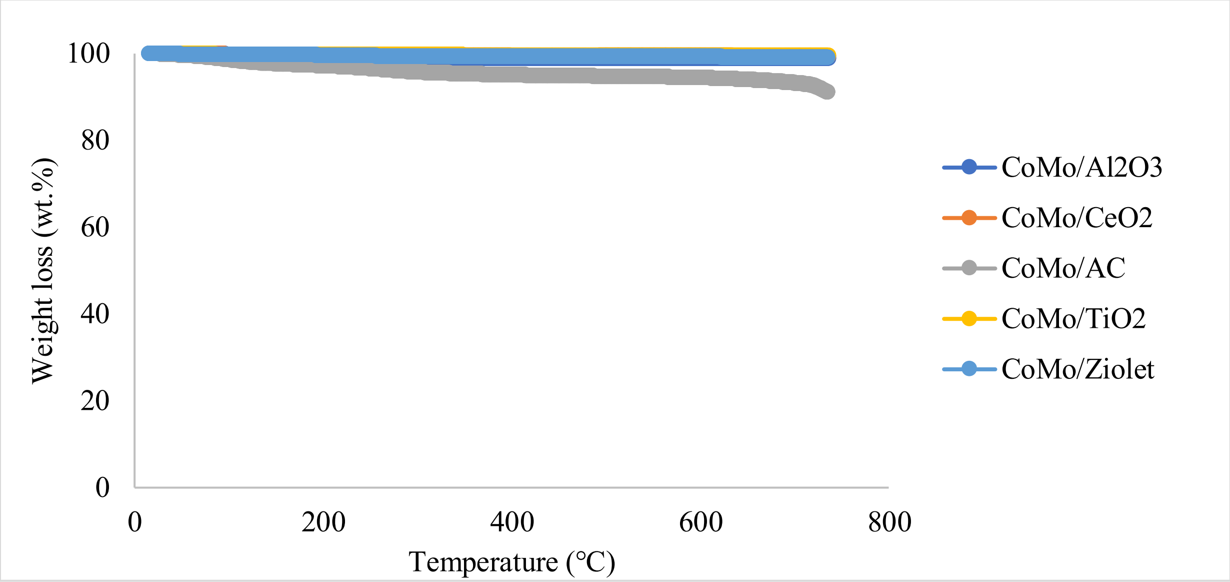

Figure 4.2. TGA profile

4.1.4. SEM Analysis

The images revealed below show the composition and various surface morphologies of the different catalysts. The needle-like structures revealed by the other catalysts were also due to the presence of non-regular fragments. This result supports previous work (F. Wang, Xu, et al., 2018). The CoMo resulted in the formation of large regular and dispersed shapes over the AC surface; meanwhile, other catalysts rendered the formation of a large flaky bulk structure with a size > 500 nm. Interestingly, the CoMo/AC catalyst led to the formation of a regular nested porous structure, which provided a patterned surface for the reaction to take place and enhanced the reaction rate by enhancing the catalytic activity. The combination of the cobalt and molybdenum with active carbon catalysts resulted in the formation of large and dispersed shapes on the AC surface. On the other hand, other catalysts created a large bulk structure with a size of over 500 nm.

(a)

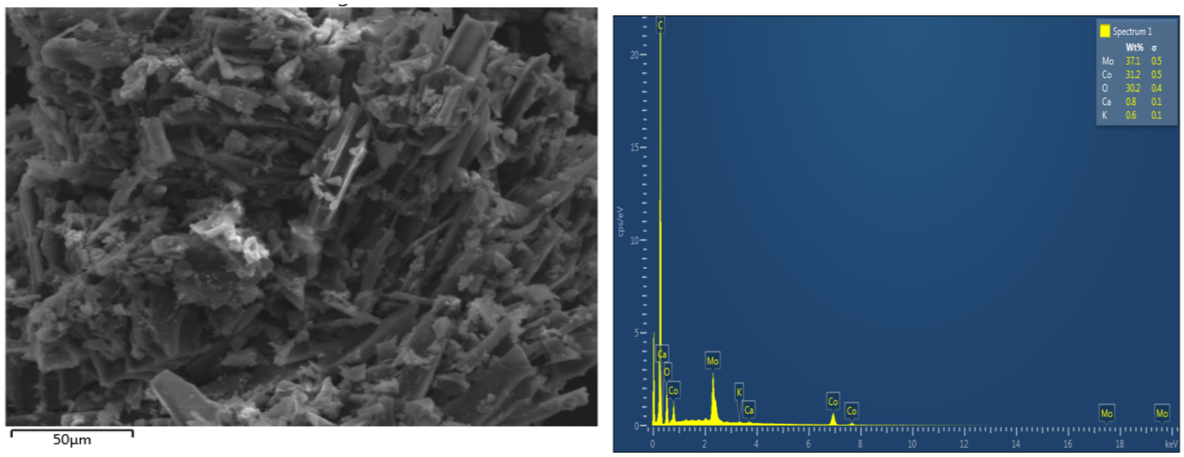
50μm
Spectrum 1
Wt% σ
Mo 37.1 0.5
Co 31.2 0.5
O 30.2 0.4
Ca 0.8 0.1
K 0.6 0.1
cps/eV
C
Ca
O
Co
Mo
K
Ca
Co
Co
Mo
Mo
0 2 4 6 8 10 12 14 16 18 keV
0 5 10 15 20

(b)

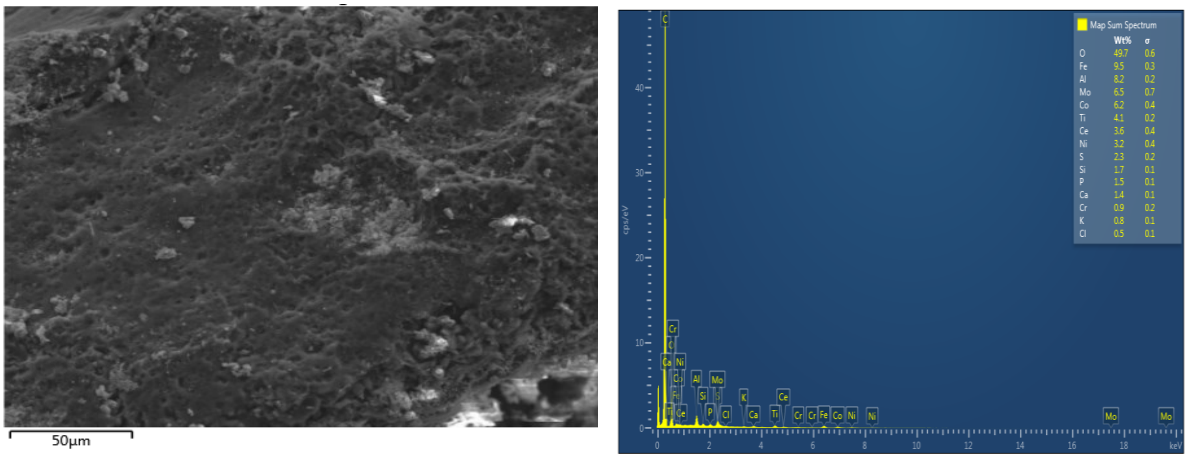
50μm
Map Sum Spectrum
Wt% σ
O 49.7 0.6
Fe 9.5 0.3
Al 8.2 0.2
Mo 6.5 0.7
Co 6.2 0.4
Ti 4.1 0.2
Ce 3.6 0.4
Ni 3.2 0.4
S 2.3 0.2
Si 1.7 0.1
P 1.5 0.1
Ca 1.4 0.1
Cr 0.9 0.2
K 0.8 0.1
Cl 0.5 0.1
cps/eV
C
Cr
O
Ca
Ni
Al
Mo
Si
S
P
Cl
K
Ca
Ti
Ce
Cr
Fe
Co
Ni
Mo
Mo
0 2 4 6 8 10 12 14 16 18 keV
0 10 20 30 40

(c)

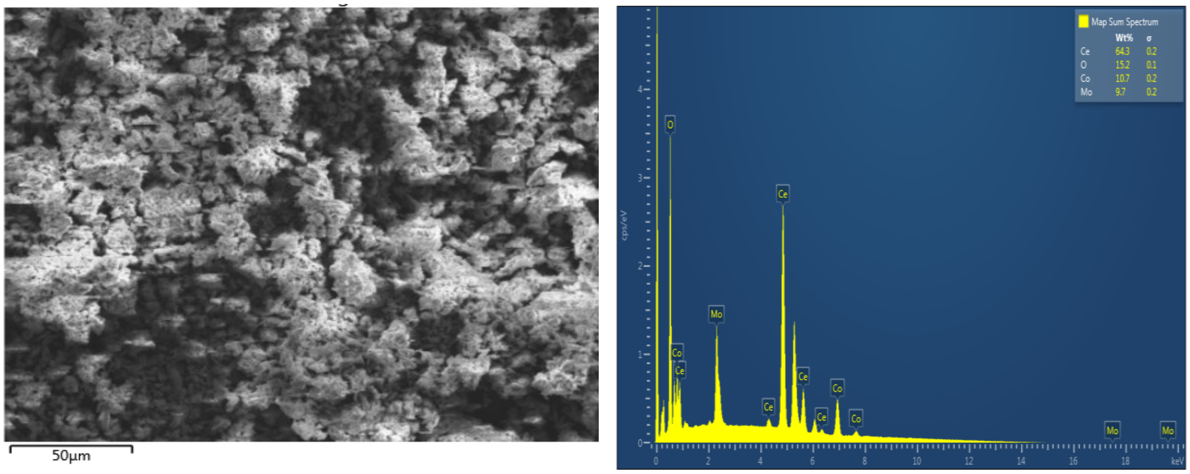
50μm
Map Sum Spectrum
Wt% σ
Ce 64.3 0.2
O 15.2 0.1
Co 10.7 0.2
Mo 9.7 0.2
cps/eV
O
Ce
Mo
Co
Ce
Ce
Ce
Co
Ce
Co
Mo
Mo
0 2 4 6 8 10 12 14 16 18 keV
0 1 2 3 4

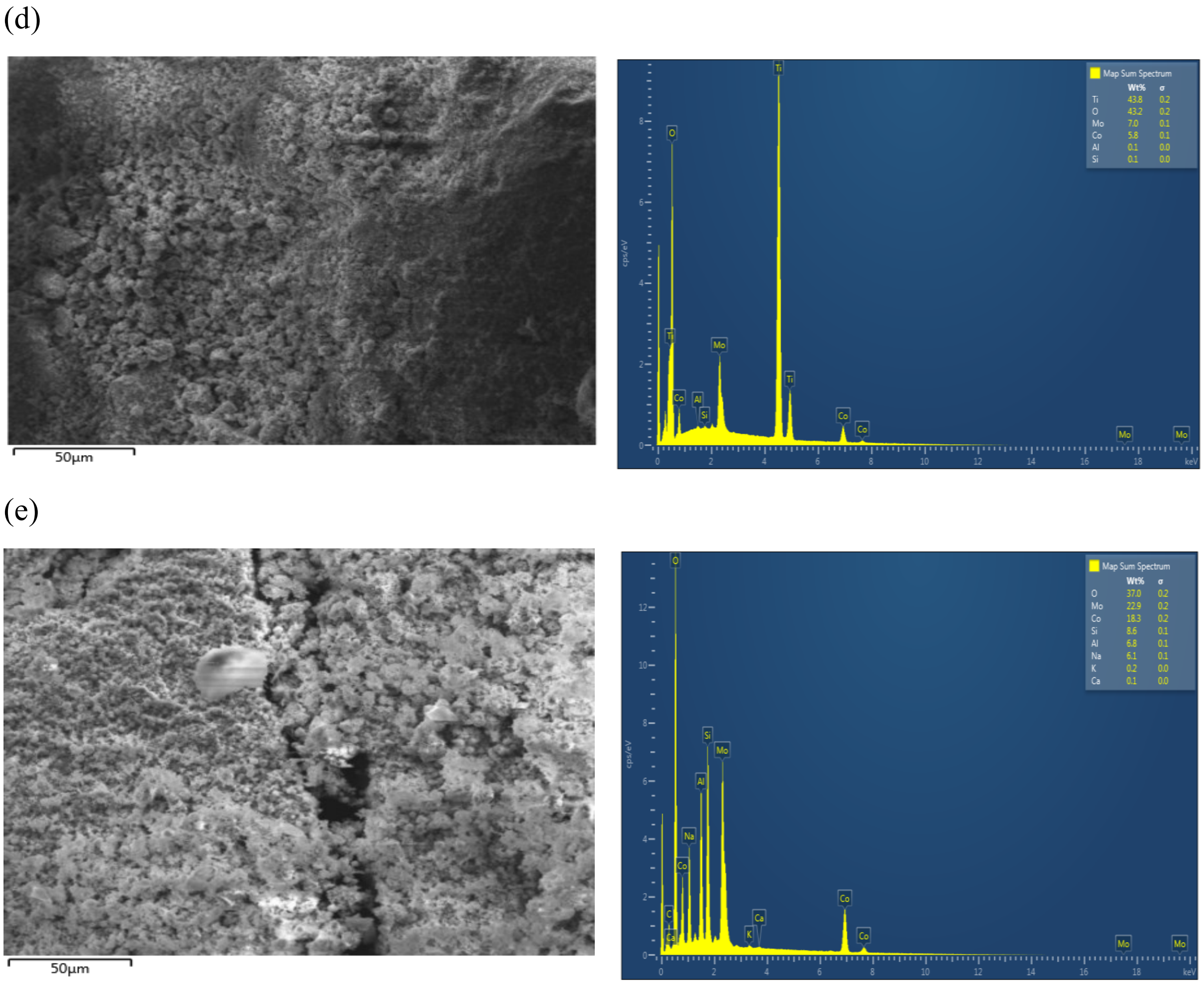

Figure 4.3. SEM image and EDX spectra of (A) Co_5Mo_5/AC, (B) Co_5Mo_5/Al_2O_3, (C) Co_5Mo_5/CeO_2, (D) Co_5Mo_5/TiO_2 (E) Co_5Mo_5/Zeolite catalyst.

The results of the EDX study revealed that the various elements of the catalysts were significantly different from one another. For instance, the cobalt and molybdenum catalysts were able to successfully attach themselves to the surface. The results of the study showed that the Mo and Co catalysts exhibited similar experimental values. Due to its exceptional mechanical and thermal properties, the activated carbon used for the deoxygenation reaction was mainly composed. This material can be used as an effective barrier during the process (F. Wang, Jiang, et al., 2018).

4.2. Catalytic Deoxygenation of Oleic Acid

4.2.1. FTIR Analysis

FTIR analysis was conducted to determine the functional groups of the blank experiment (only oleic acid without using catalyst) and deoxygenated liquid products (Figure 4.4). The dominant species in oleic acid was the oxygenated functional group derived from the ester group (C – O – C and C = O) with absorption bands at 1272 cm^{-1} and 1690 cm^{-1}. Also, aliphatic groups were present with C-H stretching at 2940 cm^{-1} and 2830 cm^{-1}. As a consequence of the deoxygenation of oleic acid, the C = O (ester) was found to shift from 1757 cm^{-1} to 1645 cm^{-1} (C = O, carboxylic acid), while the C– O group was completely eliminated. The results of the deoxygenation reaction strongly suggest that it involves breaking the bonds between the triglycerides and carboxylic acid. It can then be used to create a hydrocarbon derivative by removing the oxygen-bound species. Also, the reduction in the intensity of the carboxylic acid's C = O suggests that the CoMo/AC catalyst is more efficient in converting the carboxylic acid into oxygenate-free compound (Gamal et al., 2020). It is worth pointing out that the characteristic aliphatic C–H stretching remains unaffected.

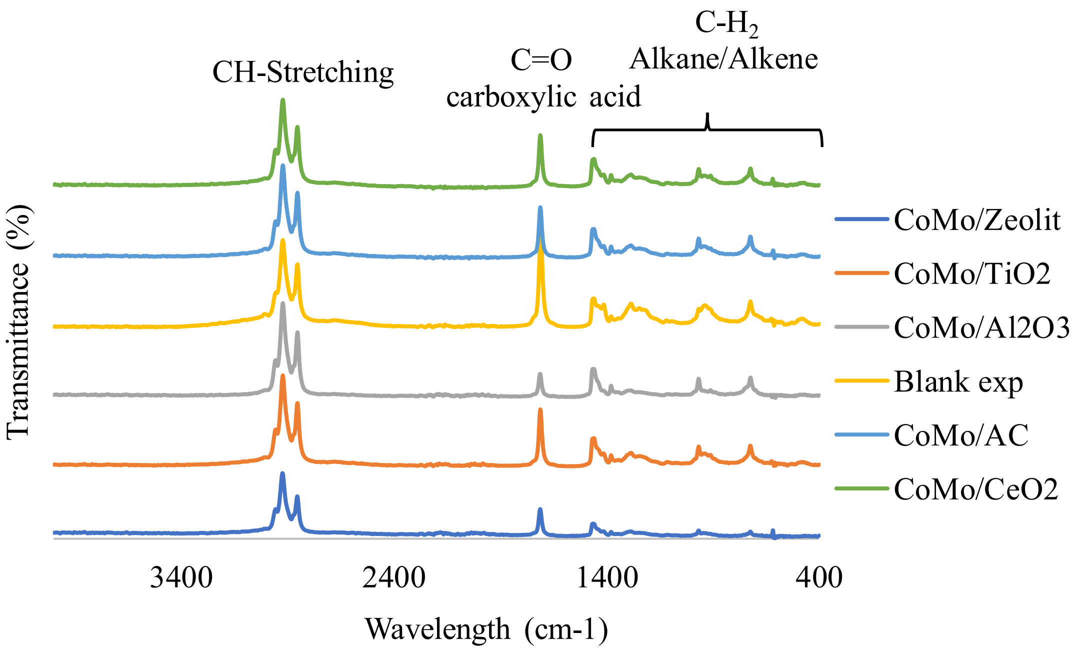

Figure 4.4. FTIR spectra of the deoxygenated liquid product

4.2.2. Gas Chromatography-Mass Spectrometry (GC-MS) Analysis

Figure 4.5 a and b show the hydrocarbon yield from catalytic deoxygenation of the oleic acid over a CoMo-based catalyst supported by Cerium oxide (CeO_2), Titanium dioxide (TiO_2), activated carbon (AC), Zeolite, and Aluminum oxide (γ-Al_2O_3) at 350 °C for 2 h reaction time using 5 wt% catalyst loading under 20 mL/min of N_2 gas flow rate. As depicted in Figure 4.5 the blank reaction experiment showed the lowest deoxygenation conversion result, this confirm the occurrence of a catalytic reaction is very necessary for the reaction.

The activated carbon (AC) supported by the CoMo-based catalyst afforded the greatest hydrocarbon yield than the other catalysts in the deoxygenation reaction. The study revealed that the presence of an active metal in the deoxygenation process of fuel-like hydrocarbons could improve the efficiency of the process. The yield of hydrocarbon increased in the order blank experiment < CoMo/TiO_2 < CoMo/CeO_2 < CoMo/Al_2O_3 < CoMo/Zeolite < CoMo/AC. Maximum hydrocarbon yield (93.20 %) was observed over CoMo/AC, suggesting that cobalt and molybdenum oxide contributed to great catalytic activity due to the high dispersion of activated carbon.

The product distribution of the deoxygenated liquid products is further analyzed by GC-MS and displayed in Figure 4.5.b |GC-MS results showed that all the catalysts lead to a higher hydrocarbon distribution (>80 %). Especially, the activated carbon-supported catalyst promoted deoxygenation activity with converting the oleic acid to hydrocarbon-like structures. The CoMo/AC catalyst showed the highest hydrocarbon distribution (93.20 %).

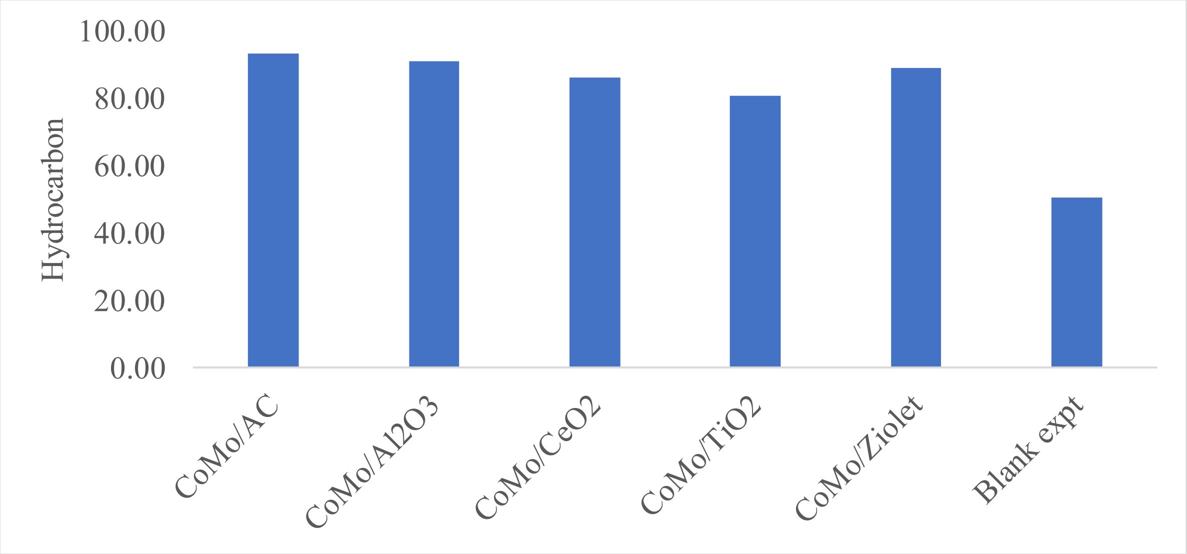

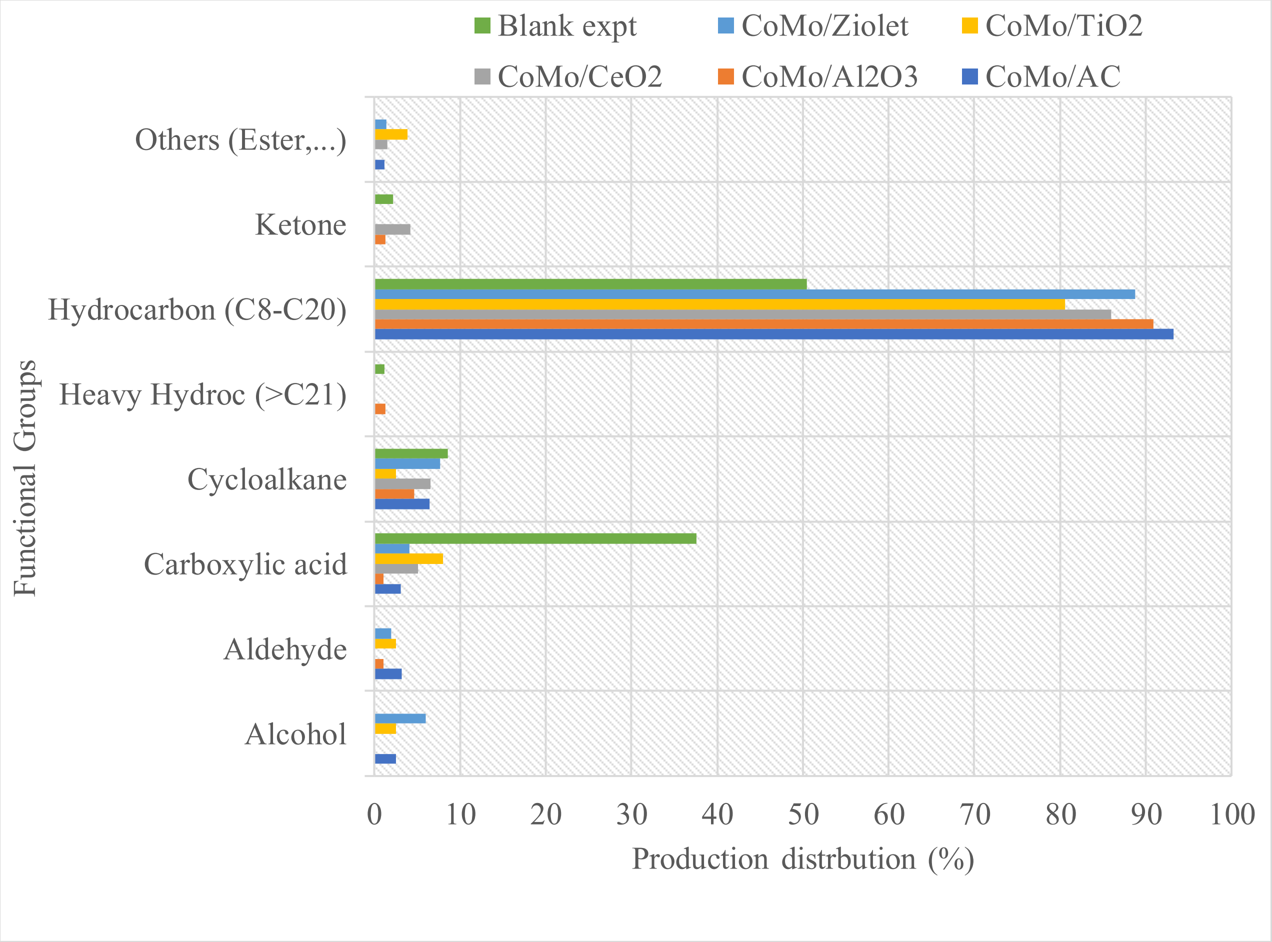

Figure 4.5. (a) production distribution and (b) Hydrocarbon yield

4.2.3. Higher Heat Value Analysis

Higher heat value indicates the energy present in the fuel and defines the efficiency of the fuel. Figure 4.6 shows the heat value of all the green diesel produced by catalyzed deoxygenation of oleic acid over CoMo/TiO_2, CoMo/CeO_2, CoMo/Al_2O_3, CoMo/Zeolite, and CoMo/AC. Especially the HHV value of CoMo/AC where the value (49.64 MJ/kg) is close to Liquefied petroleum gas and the other HHV values are close to ULSD specifications (42 - 46 MJ kg). The green diesel exhibited higher HV than the standard ULSD. Thus, green diesel can show a better energy efficiency with lower CO_2 emissions (Douvartzides et al., 2019). Depending on the HHV results it can be said that CoMo/AC showed a good catalytic performance than others.

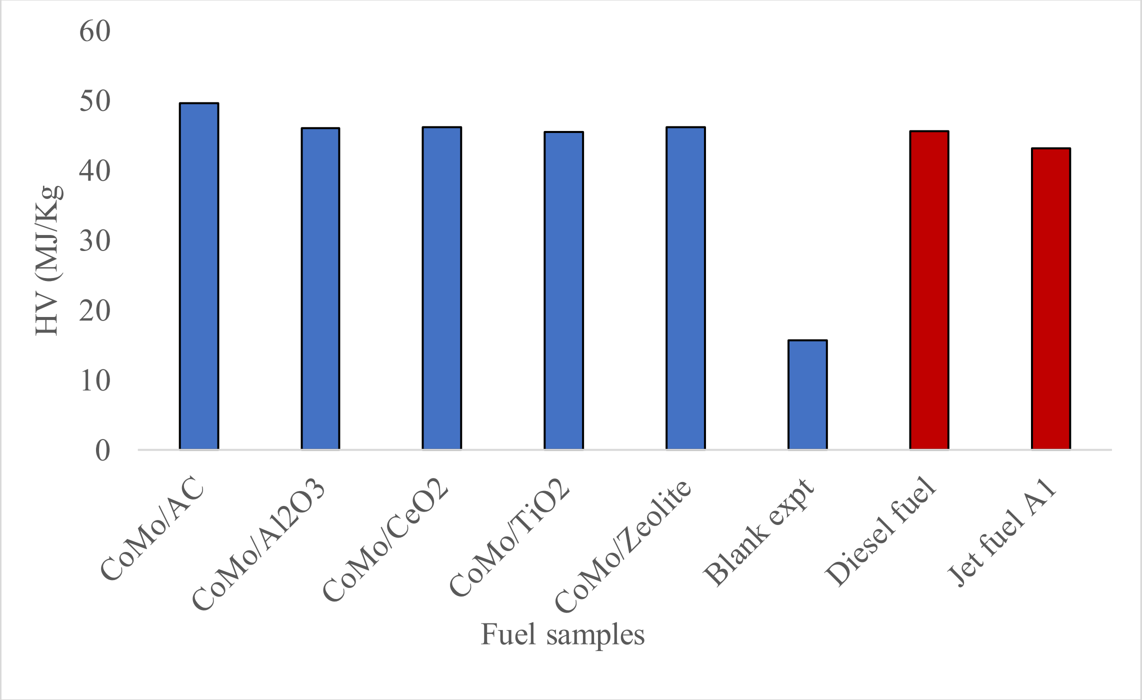

Figure 4.6. HHV result for black and green diesel obtained from oleic acid deoxygenation reaction over $CoMo/TiO_2$, $CoMo/CeO_2$, $CoMo/Al_2O_3$, CoMo/Zeolite and CoMo/AC catalysts.

4.2.4. CHNOS Analysis of The Deoxygenated Liquid Product

The elemental analysis of carbon, hydrogen, and oxygen was conducted by CHNOS analysis and it permitted to predict the effect of the catalysts in the deoxygenation process. The outcomes are represented in terms of H/C and O/C atomic ratios in the Van Krevelen diagram (Figure 4.7 below). The blank experiment H/C ratio is 1.499, while the O/C ratio is 0.1995. As we anticipated, this showed that the blank experiment contained the highest volume of oxygen. In any case, all of the catalyzed deoxygenized liquid products showed a lower O/C atomic ratio in the range 0.087– 0.183, even lower than the blank.

In this experiment, we investigate the elimination of oxygenated compounds that were accelerated by the presence of the catalyst. Remarkably, the blank reaction showed the lowest H/C atomic ratio and the highest O/C atomic ratio 1.499 and 0.1995 respectively. This is most likely because of the high cracking activities (Ibadurrohman et al., 2022).

Generally, the rate of C–O bond cleavage is less affected by the blank reaction than the rate of C–C bond cleavage. Among the catalyzed reactions, the CoMo/AC catalyst displays the second-least O/C ratio (0.091) after the $CoMo/Al_2O_3$ and the highest H/C ratio (1.564).

Presumably, CoMo/AC affords an excellent oxygenate removal efficiency along with an outstanding saturation of double bonds (Santillan-Jimenez & Crocker, 2012), thus producing fuels rich in paraffinic hydrocarbons. The results of the study are in agreement with those of the GC-MS analysis, which showed that the presence of paraffinic species was high. The blank experiment exhibited a lower H/C ratio and a greater O/C ratio than the whole catalysts.

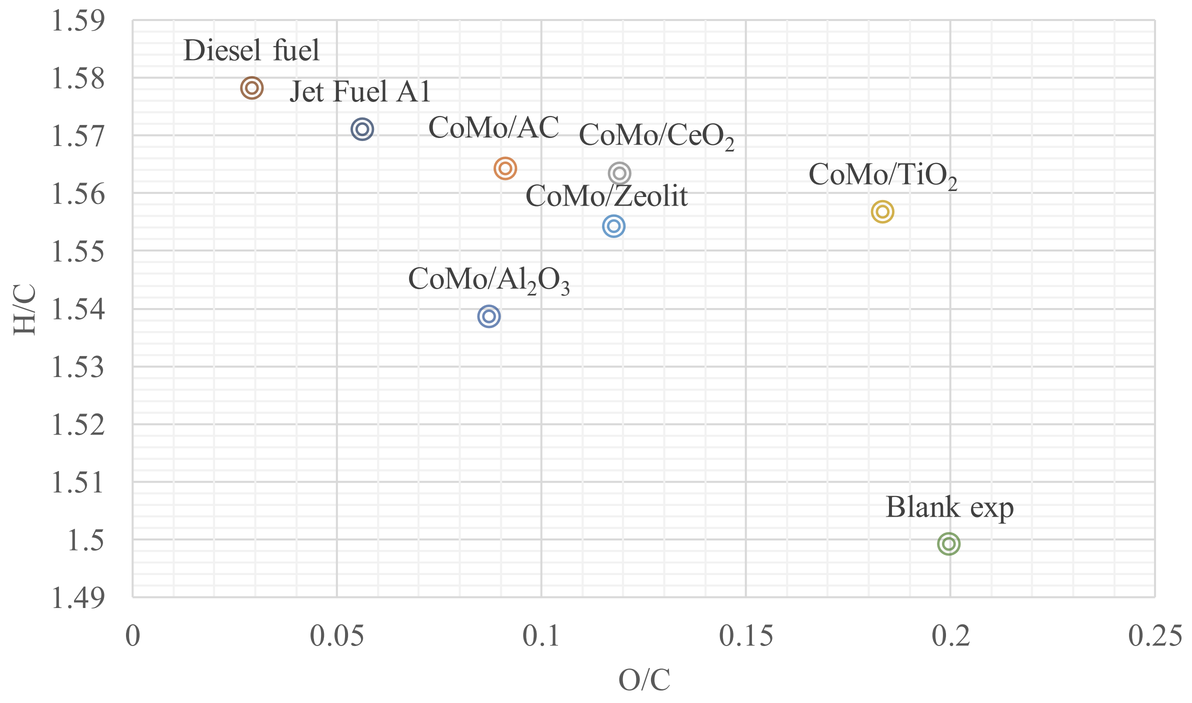

Figure 4.7. Van Krevelen diagram for H/C & O/C ratio of the blank exp and DO liquid products

5. SIMULATION OF DEOXYGENATİON REACTİON USİNG SUPERPRO DESİGNER SOFTWARE

5.1. Introduction For Process Simulation and Economic Modeling

One of the most powerful tools for decision-makers is simulation. It allows them to design and evaluate various environmental and manufacturing processes in the same package. This allows them to practice waste minimization and pollution prevention. Before a process can be commercialized, a comprehensive analysis of the economic feasibility and design requirements is required. With the ability to study and evaluate complex systems and processes, simulation has become an integral part of every decision-making process. It allows engineers, designers, and managers to make informed decisions and improve their efficiency.

SuperPro Designer is a powerful tool for scientists and engineers who are involved in process engineering and manufacturing. It can help them develop effective strategies and manage environmental issues related to their work. It can also help them predict the impact of their projects on the environment. SuperPro Designer can help engineers and scientists develop effective strategies and manage their projects' environmental impact. It can be used in various industries such as pharmaceutical, biotechnology, and food.

In this study, the concept of deoxygenation of oleic acid using SuperPro Designer was presented. The resulting design was then validated with a simulation that shows the production of green diesel, which is produced from non-edible oil, at a rate of 2,975.09 cubic meters per year. There is a great interest to produce renewable fuels, such as green diesel. This fuel is made from the alkyl compounds found in agricultural oils and fats. Producing green diesel from vegetable fats and oils has been shown to give engines similar performance to that of conventional fuels. It can also be produced using animal fats or vegetable oils. The choice is also limited by the availability of these materials and the government's regulations.

Here are the three most dominant ways of green diesel production:

- Deoxygenation
- HDO (Hydrodeoxygenation) and
- Pyrolysis

5.2. Process Description of The Simulation

For simplification purposes, the process has been split into three sections: The Reaction (red icons), the upstream process (blue icons), and the downstream process (violet icons) section. A section in SuperPro is simply a set of unit procedures (processing steps).

The reaction section consists of:

- The raw material storage tanks for the oil (TNK-101) and the catalyst transfer by pneumatic conveyer (PC-101)
- The semi-batch reactors (R-101)
- A flash separator (V-101)

The oil and the catalyst are directly fed to the reactor (R-101) and mixed by the agitator in the reactor. According to the reaction mentioned in the super pro reaction operation data, the reactor temperature gradually raised to 350 °C with constant stirring (300 rpm) and with average residence time of materials in the reaction is under 20 mL/min of N_2 gas flow rate to yield green diesel and glycerol. Product is removed at a rate of twice to the rate of charging the reactants. The material is then fed to a flash separator (V-101) where the green diesel and the oil that has not reacted are separated with catalyst from the glycerol rich co-product phase.

NB: - The amount of all raw matrials in this process are based on the labratory result.

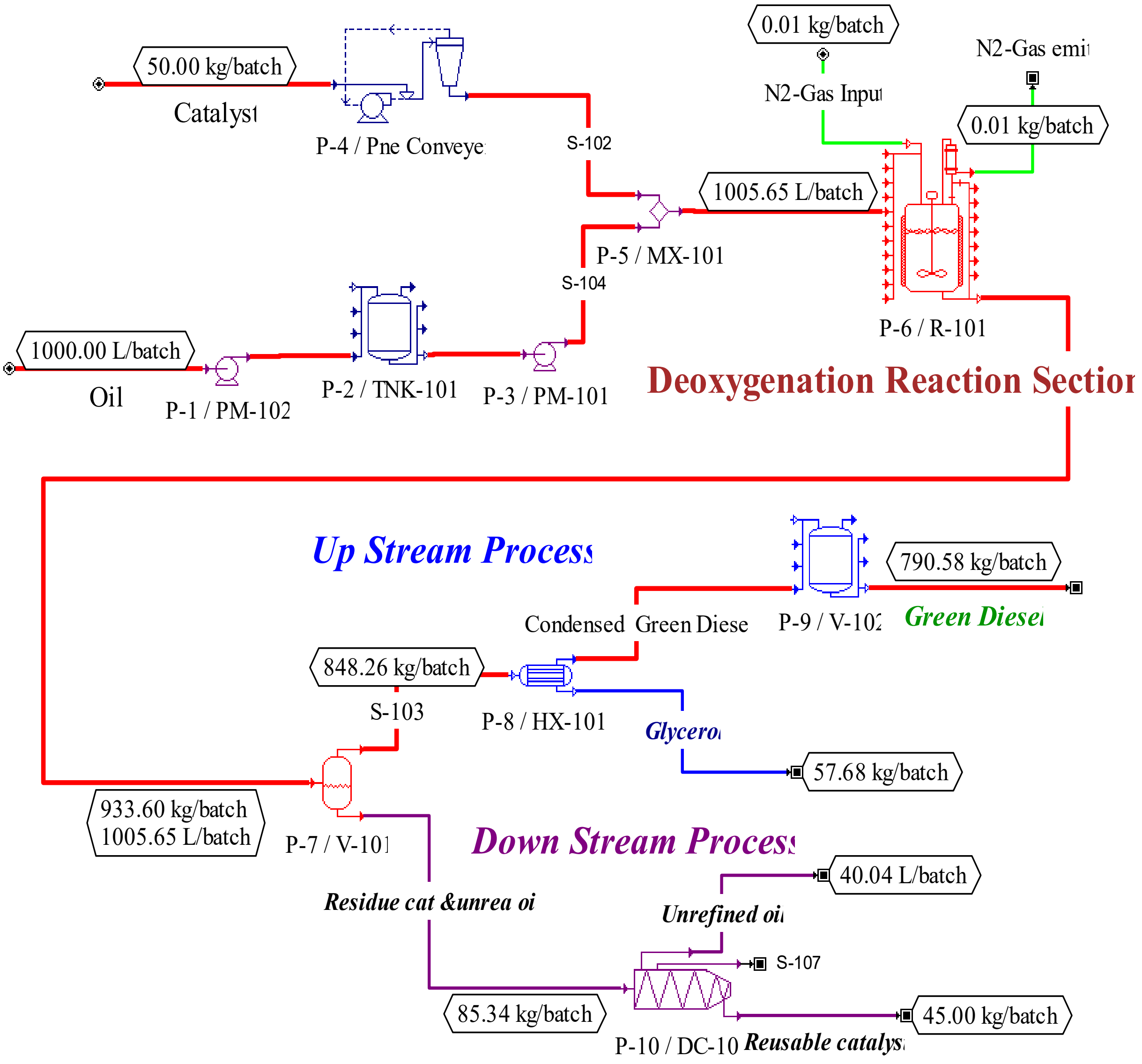

Figure 5.1. SuperPro Designer Process flowsheet for deoxygenation of oleic acid to obtain green diesel

5.3. Raw Material Requirements

The table below displays the raw material requirements in kg/h, kg/year, and kg/kg MP (main product – green diesel in this case). This plant produces approximately 2,975.09 cubic meters per year of green diesel and 189.02 ton of glycerol per year. The table below was extracted from the RTF version of the Streams & Mat. Balance report, which can be generated by selecting Reports \ Streams & Mat. Balance from the main menu bar of SuperPro. The format of the report can be specified through the dialog that is displayed when we select Reports \ Options from the main menu bar of SuperPro.

Table 5.1. Raw Material Requirements for the production of diesel

Bulk Materials (Entire Process)			
Material	**kg/yr**	**kg/batch**	**kg/kg MP**
Catalyst	163850.00	50.00	0.06
Nitrogen	22.51	0.01	0.00
Oleic Acid	2895569.09	883.60	1.12
TOTAL	**3059441.60**	**933.61**	**1.18**

5.4. Economic Evaluation

The estimated economic output of a proposed plant that would produce 2,975.09 cubic meters of green diesel per year is shown in the table below. The total capital investment for a plant of around 586,000 $ is computed by considering the annual operating costs and the unit production cost. This value is computed by considering the annual operating costs (around $3.4 million) and the unit production cost (around $1.34/kg). The project life of the plant is estimated to be 15 years. The revenues are based on a selling price of $1.45/kg. Revenues of around $0.14 million are generated from the sale of glycerol the by-product of this process. The profitability of a venture involving the production of green diesel depends on the price of oil that's used to make the fuel and the level of government subsidies that it receives.

Table 5.2. Executive summary for the production of diesel

Executive Summary (2022 prices)		
Total Capital Investment	586,000	$
Capital Investment Charged to This Project	586,000	$
Operating Cost	3,476,000	$/yr
Net Operating Cost	3,475,510	$/yr
Main Revenue	3,757,000	$/yr
Other Revenues	178,633	$/yr
Total Revenues	3,935,000	$/yr
Cost Basis Annual Rate	2,590,724	kg MP/yr
Unit Production Cost	1.34	$/kg MP
Net Unit Production Cost	1.34	$/kg MP
Unit Production Revenue	1.52	$/kg MP
Gross Margin	11.68	%
Return On Investment	55.22	%
Payback Time	1.81	years
IRR (After Taxes)	35.70	%
NPV (at 7.0% Interest)	1,811,000	$

MP = Total Flow of Stream 'Green Diesel'

Table 5.3. Equipment specification and their cost

Major Equipment Specification And FOB Cost (2022 Prices)

Quantity/ Standby/ Staggered	**Name**	**Description**	**Unit Cost ($)**	**Cost ($)**
1 / 2 / 0	PM-101	Centrifugal Pump Pump Power = 0.16 kW	1,000	3,000
1 / 0 / 0	PC-101	Pneumatic Conveyor Pipe Length = 150.00 m	1,000	1,000
1 / 0 / 0	R-101	Stirred Reactor Vessel Volume = 1117.39 L	10,000	10,000
1 / 0 / 0	V-101	Flash Drum Vessel Volume = 556.46 L	7,000	7,000
1 / 0 / 0	DC-101	Decanter Centrifuge Throughput = 182.48 L/h	4,000	4,000
1 / 0 / 0	HX-101	Condenser Condensation Area = 0.00 m2	5,000	5,000
1 / 0 / 0	V-102	Receiver Tank Vessel Volume = 1008.74 L	5,000	5,000
1 / 0 / 0	TNK-101	Receiver Tank Vessel Volume = 1111.13 L	5,000	5,000
1 / 0 / 0	PM-102	Centrifugal Pump Pump Power = 0.16 kW	1,000	1,000
		Unlisted Equipment		9,000
			TOTAL	**47,000**

Table 5.4. Fixed capital investment cost

Fixed Capital Estimate Summary (2022 Prices in $)	
3A. Total Plant Direct Cost (TPDC) (physical cost)	
1. Equipment Purchase Cost	47,000
2. Installation	20,000
3. Process Piping	14,000
4. Instrumentation	17,000
5. Insulation	1,000
6. Electrical	5,000
7. Buildings	19,000
8. Yard Improvement	7,000
9. Auxiliary Facilities	19,000
TPDC	149,000
3B. Total Plant Indirect Cost (TPIC)	
10. Engineering	34,000
11. Construction	45,000
TPIC	79,000
3C. Total Plant Cost (TPC = TPDC+TPIC)	
TPC	227,000
3D. Contractor's Fee & Contingency (CFC)	
12. Contractor's Fee	11,000
13. Contingency	23,000
CFC = 12+13	34,000
3E. Direct Fixed Capital Cost (DFC = TPC+CFC)	
DFC	**261,000**

The table below shows the annual operating cost of a facility. The most important item is the raw materials cost, which is the price of oil. The other cost items include the facility-dependent cost, which is the cost of maintaining the facility, and the cost of utilities.

Table 5.5. Manufacturing cost breakdown for diesel process

Annual Operating Cost (2022 Prices) – Process Summary		
Cost Item	**$**	**%**
Raw Materials	2,543,000	73.18
Labor-Dependent	554,000	15.93
Depreciation	25,000	0.71
Other Facility-Dependent	25,000	0.71
Consumables	0	0
Waste Treatment/Disposal	0	0
Utilities	329,000	9.47
Transportation	0	0
Miscellaneous	0	0
Advertising/Selling	0	0
Running Royalties	0	0
Failed Product Disposal	0	0
TOTAL	3,476,000	100

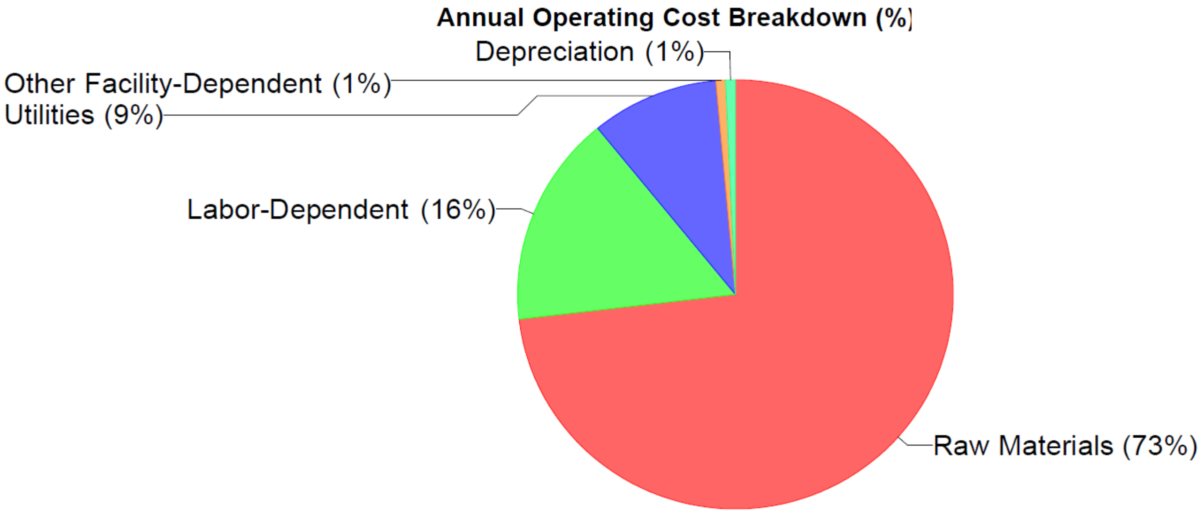

Figure 5.2. Manufacturing cost breakdown for diesel process by chart

Table 5.6. The deoxygenized liquid product profitability analysis

Profitability Analysis (2022 prices)			
A.	Direct Fixed Capital	261,000	$
B.	Working Capital	311,000	$
C.	Startup Cost	13,000	$
D.	Up-Front R&D	0	$
E.	Up-Front Royalties	0	$
F.	Total Investment (A+B+C+D+E)	586,000	$
G.	Investment Charged to This Project	586,000	$
H.	**Revenue/Savings Rates**		
	Glycerol (Revenue)	189,023	kg /yr.
	Reusable catalyst (Revenue)	147,465	kg /yr.
	Green Diesel (Main Revenue)	2,879,817	L(STP) /y
I.	**Revenue/Savings Price**		
	Glycerol (Revenue)	0.75	$/kg
	Reusable catalyst (Revenue)	0.25	$/kg
	Green Diesel (Main Revenue)	1.30	$/L(STP)
J.	**Revenues/Savings**		
	Glycerol (Revenue)	141,767	$/yr.
	Reusable catalyst (Revenue)	36,866	$/yr.
	Green Diesel (Main Revenue)	3,756,549	$/yr.
1	Total Revenues	3,935,182	$/yr.
2	Total Savings	0	$/yr.
K.	**Annual Operating Cost (AOC)**		
	Actual AOC w/out Depreciation	3,451,000	$/yr.
	Net AOC w/out Depreciation	3,451,000	$/yr.
1	Actual AOC with Depreciation	3,476,000	$/yr.
2	Net AOC with Depreciation (K1-J2)	3,476,000	$/yr.
L.	**Unit Production Cost /Revenue**		
	Unit Production Cost (w/out depreciation)	1.33	$/kg MP
	Net Unit Production Cost (w/out depreciation)	1.33	$/kg MP
	Unit Production Cost (w/out depreciation)	1.34	$/kg MP
	Net Unit Production Cost (w/out depreciation)	1.34	$/kg MP
	Unit Production Revenue	1.52	$/kg MP
M.	Gross Profit (J-K)	460,000	$/yr.
N.	Taxes (35%)	161,000	$/yr.
O.	Net Profit (M-N + Depreciation)	324,000	$/yr.
	Gross Margin	**11.68**	**%**
	Return On Investment	**55.22**	**%**
	Payback Time	**1.81**	**years**

5.5. Process Scheduling

SuperPro design software is also generates **Equipment** and **Operations Gantt Charts** for multiple batches. The following figure displays the portion of the operations chart that shows the start, duration, and end time of a single process. The left view shows the name, duration, and end time of each activity (some of them are each individual operation, unit procedure, cycle, batch, etc.). The left view displays the summaries of all the activities that are related to a given batch by clicking on + or – signs in the boxes. The operations Gantt chart can be used to visualize the various steps and procedures that are involved in a given process. This chart is very important in determining the annual capacity of a particular batch.

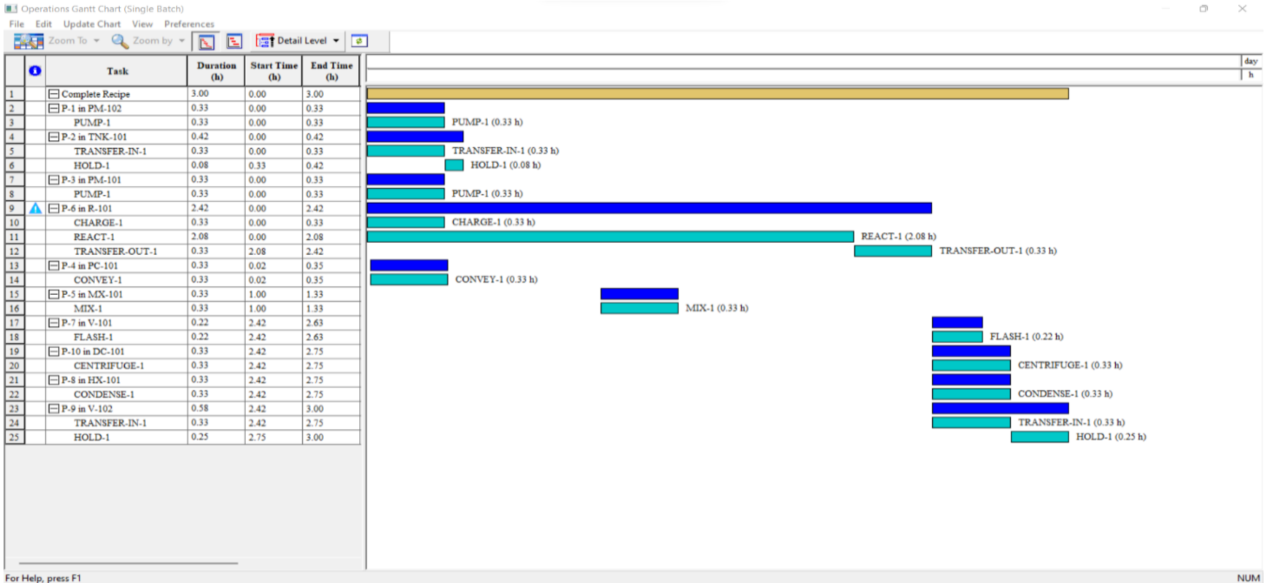

	ⓘ	Task	Duration (h)	Start Time (h)	End Time (h)
1		⊟ Complete Recipe	3.00	0.00	3.00
2		⊟ P-1 in PM-102	0.33	0.00	0.33
3		PUMP-1	0.33	0.00	0.33
4		⊟ P-2 in TNK-101	0.42	0.00	0.42
5		TRANSFER-IN-1	0.33	0.00	0.33
6		HOLD-1	0.08	0.33	0.42
7		⊟ P-3 in PM-101	0.33	0.00	0.33
8		PUMP-1	0.33	0.00	0.33
9	⚠	⊟ P-6 in R-101	2.42	0.00	2.42
10		CHARGE-1	0.33	0.00	0.33
11		REACT-1	2.08	0.00	2.08
12		TRANSFER-OUT-1	0.33	2.08	2.42
13		⊟ P-4 in PC-101	0.33	0.02	0.35
14		CONVEY-1	0.33	0.02	0.35
15		⊟ P-5 in MX-101	0.33	1.00	1.33
16		MIX-1	0.33	1.00	1.33
17		⊟ P-7 in V-101	0.22	2.42	2.63
18		FLASH-1	0.22	2.42	2.63
19		⊟ P-10 in DC-101	0.33	2.42	2.75
20		CENTRIFUGE-1	0.33	2.42	2.75
21		⊟ P-8 in HX-101	0.33	2.42	2.75
22		CONDENSE-1	0.33	2.42	2.75
23		⊟ P-9 in V-102	0.58	2.42	3.00
24		TRANSFER-IN-1	0.33	2.42	2.75
25		HOLD-1	0.25	2.75	3.00

Figure 5.3. Operations Gantt chart for single batch

5.6. Plant Site Selection

The location of a plant is also important when it comes to deciding where it should be built. For instance, in the case of the oil and gas project, the location of the plant should be in the region of Gambela. Various factors can be considered when it comes to establishing a plant, such as the availability of skilled workers and power supply from the construction of the Ethiopia Renascence Dam, and also the infrastructures like the international (Ethio-Sudan) road. There are also various transportation options to access the raw material that can be considered such as the border of Sudan or the capital city of Addis Ababa.

6. CONCLUSION AND RECOMMENDATIONS

6.1. Conclusion

In this study, the catalytic deoxygenation of oleic acid to green diesel under solvent-free conditions was investigated over CoMo/AC, CoMo/Al_2O_3, CoMo/CeO_2, CoMo/TiO_2, and CoMo/Zeolite catalysts. Among the catalysts tested, CoMo/AC exhibited promising activity with the highest hydrocarbon yield (93.20%) obtained under optimum conditions of 5 wt.% amount of catalyst, 350 °C of the reaction temperature, and with a 120 min reaction time. The reaction performance increased by high surface area, smaller crystallization size, and high pore volume. CoMo catalyst supported on AC showed the high effectiveness and catalytic deoxygenation activity to supply the formation of green diesel range products. At the same time, the Co_5Mo_5/AC catalyst is low cost with environmentally friendly. Therefore, from the SuperPro designer simulation study this project is feasible because it requires low capital investment (payback period ≈1.8 years), less complex manufacturing process and low energy consumption.

6.2. Recommendations

To study the efficiency of the deoxygenation process in real-world conditions, studies should be carried out on the various steps involved in this process. One of these is to determine the optimal strategy for optimizing the production of green diesel by continuously operating a reactor. This method would minimize the chances of encountering issues during the production phase. Studies on the effects of various synthesis parameters on the structure and performance of monometallic catalysts are recommended. In addition, engine tests are also recommended for green diesel that is produced through a deoxygenation reaction. The studies on the various operational and financial aspects of the process are expected to be carried out in the future. The studies on the price of vegetable oil and its impact on the profitability of the process are also expected to be conducted.

REFERENCES

Abdulkareem-Alsultan, G., Asikin-Mijan, N., Lee, H. V., and Taufiq-Yap, Y. H. (2016). A new route for the synthesis of La-Ca oxide supported on nano activated carbon via vacuum impregnation method for one pot esterification-transesterification reaction. Chemical Engineering Journal, 304, 61–71.

Afshar Taromi, A., and Kaliaguine, S. (2018). Green diesel production via continuous hydrotreatment of triglycerides over mesostructured γ-alumina supported NiMo/CoMo catalysts. Fuel Processing Technology, 171, 20–30.

Alsultan, G. A., Asikin-Mijan, N., Lee, H. V., Albazzaz, A. S., and Taufiq-Yap, Y. H. (2017). Deoxygenation of waste cooking to renewable diesel over walnut shell-derived nanorode activated carbon supported CaO-La2O3 catalyst. Energy Conversion and Management, 151, 311–323.

Anwar, M., Khan, H., Bonifacio, S., Clowes, J., Foulds, A., Holland, R., Matthews, J. C., Percival, C. J., Shallcross, D. E., and Karavalakis, G. (2021). Investigation of Biofuel as a Potential Renewable Energy Source. MDPI.

Asikin-Mijan, N., Lee, H. V., Juan, J. C., Noorsaadah, A. R., Abdulkareem-Alsultan, G., Arumugam, M., and Taufiq-Yap, Y. H. (2016). Waste clamshell-derived CaO supported Co and W catalysts for renewable fuels production via cracking-deoxygenation of triolein. Journal of Analytical and Applied Pyrolysis, 120, 110–120.

Asikin-Mijan, N., Lee, H. V., Abdulkareem-Alsultan, G., Afandi, A., and Taufiq-Yap, Y. H. (2017). Production of green diesel via cleaner catalytic deoxygenation of Jatropha curcas oil. Journal of Cleaner Production, 167, 1048–1059.

Asikin-Mijan, N., Lee, H. V., Taufiq-Yap, Y. H., Juan, J. C., and Rahman, N. A. (2016). Pyrolytic–deoxygenation of triglyceride via natural waste shell derived Ca(OH)2 nanocatalyst. Journal of Analytical and Applied Pyrolysis, 117, 46–55.

Bernas, H., Eränen, K., Simakova, I., Leino, A. R., Kordás, K., Myllyoja, J., Mäki-Arvela, P., Salmi, T., and Murzin, D. Y. (2010). Deoxygenation of dodecanoic acid under inert atmosphere. Fuel, 89/8, 2033–2039.

BP Energy. (2019). Statistical Review of World Energy globally consistent data on world energy markets . and authoritative publications in the field of energy. In BP Energy outlook 2019 (Vol. 70, pp. 8–20).

Da Mota, S. D. P., Mancio, A. A., Lhamas, D. E. L., De Abreu, D. H., Da Silva, M. S., Dos Santos, W. G., De Castro, D. A. R., De Oliveira, R. M., Araújo, M. E., Borges, L. E. P., and Machado, N. T. (2014). Production of green diesel by thermal catalytic cracking of crude palm oil (Elaeis guineensis Jacq) in a pilot plant. Journal of Analytical and Applied Pyrolysis, 110/1, 1–11.

Di Vito Nolfi, G., Gallucci, K., and Rossi, L. (2021). Results for "Di Vito Nolfi, G., Gallucci, K., & Rossi, L. (2021). Green diesel production by catalytic hydrodeoxygenation of vegetables oils. In International Journal of Environmental Research and Public Health (Vol. 18, Issue 24). MDPI. https://doi.org/1. In International Journal of Environmental Research and Public Health (Vol. 18, Issue 24). MDPI.

Douvartzides, S. L., Charisiou, N. D., Papageridis, K. N., and Goula, M. A. (2019). Green Diesel: Biomass Feedstocks, Production Technologies, Catalytic Research, Fuel Properties and Performance in Compression Ignition Internal Combustion Engines.

Fangkoch, S., Boonkum, S., Ratchahat, S., Koo-Amornpattana, W., Eiad-Ua, A., Kiatkittipong, W., Klysubun, W., Srifa, A., Faungnawakij, K., and Assabumrungrat, S. (2020). Solvent-Free Hydrodeoxygenation of Triglycerides to Diesel-like Hydrocarbons over Pt-Decorated MoO 2

Catalysts.

Gamal, M. S., Asikin-Mijan, N., Khalit, W. N. A. W., Arumugam, M., Izham, S. M., and Taufiq-Yap, Y. H. (2020). Effective catalytic deoxygenation of palm fatty acid distillate for green diesel production under hydrogen-free atmosphere over bimetallic catalyst CoMo supported on activated carbon. Fuel Processing Technology, 208, 106519.

Gaurav, A., Dumas, S., Mai, C. T. Q., and Ng, F. T. T. (2019). A kinetic model for a single step biodiesel production from a high free fatty acid (FFA) biodiesel feedstock over a solid heteropolyacid catalyst. Green Energy and Environment, 4/3.

Gielen, D., Boshell, F., Saygin, D., Bazilian, M. D., Wagner, N., and Gorini, R. (2019). The role of renewable energy in the global energy transformation. Energy Strategy Reviews, 24, 38–50.

Gosselink, R. W., Hollak, S. A. W., Chang, S.-W., Van Haveren, J., De Jong, K. P., Bitter, J. H., and Van Es, D. S. (2013). Reaction Pathways for the Deoxygenation of Vegetable Oils and Related Model Compounds. Wiley-VCH Verlag GmbH & Co. KGaA, Weinheim, 1576–1594.

Hermida, L., Abdullah, A. Z., and Mohamed, A. R. (2015). Deoxygenation of fatty acid to produce diesel-like hydrocarbons: A review of process conditions, reaction kinetics and mechanism. In Renewable and Sustainable Energy Reviews (Vol. 42).

Hsu, P. J., and Lin, Y. C. (2017). Hydrodeoxygenation of 4-methylguaiacol over silica-supported nickel phosphide catalysts: The particle size effect. Journal of the Taiwan Institute of Chemical Engineers, 79, 80–87.

Ibadurrohman, I. A., Hamidi, N., and Yuliati, L. (2022). The role of the unsaturation degree on the droplet combustion characteristics of fatty acid methyl ester. Alexandria Engineering Journal, 61/3, 2046–2060.

Ikram, M., Ferasso, M., Sroufe, R., and Zhang, Q. (2021). Assessing green technology indicators for cleaner production and sustainable investments in a developing country context. Journal of Cleaner Production, 322, 129090.

Jain, A., Ong, V., Jayaraman, S., Balasubramanian, R., and Srinivasan, M. P. (2016). Supercritical fluid immobilization of horseradish peroxidase on high surface area mesoporous activated carbon. The Journal of Supercritical Fluids, 107, 513–518.

Janampelli, S., and Darbha, S. (2018). Selective and reusable Pt-WOx/Al2O3 catalyst for deoxygenation of fatty acids and their esters to diesel-range hydrocarbons. Catalysis Today, 309, 219–226.

Kebede, L., Tulu, G. S., and Lisinge, R. T. (2022). Diesel-fueled public transport vehicles and air pollution in Addis Ababa, Ethiopia: Effects of vehicle size, age and kilometers travelled. Atmospheric Environment: X, 13, 100144.

Krobkrong, N., Itthibenchapong, V., Khongpracha, P., and Faungnawakij, K. (2018). Deoxygenation of oleic acid under an inert atmosphere using molybdenum oxide-based catalysts. Energy Conversion and Management, 167, 1–8.

Kwon, K. C., Mayfield, H., Marolla, T., Nichols, B., and Mashburn, M. (2011). Catalytic deoxygenation of liquid biomass for hydrocarbon fuels. Renewable Energy, 36/3, 907–915.

Lestari, S., Mäki-Arvela, P., Simakova, I., Beltramini, J., Lu, G. Q. M., and Murzin, D. Y. (2009). Catalytic deoxygenation of stearic acid and palmitic acid in semibatch mode. Catalysis Letters, 130/1–2, 48–51.

Liu, M., Zhou, L., Luo, X., Wan, C., and Xu, L. (2020). Recent advances in noble metal catalysts for hydrogen production from ammonia borane. Catalysts, 10/7, 1–34.

Liu, Z.-H., Hao, N., Wang, Y.-Y., Dou, C., Lin, F., Shen, R., Bura, R., Hodge, D. B., Dale, B. E., Ragauskas, A. J., Yang, B., and Yuan, J. S. (2021). Transforming biorefinery designs with "Plug-In Processes of Lignin" to enable economic waste valorization. Nature Communications.

Mäki-Arvela, P., Kubickova, I., Snåre, M., Eränen, K., and Murzin, D. Y. (2007). Catalytic deoxygenation of fatty acids and their derivatives. Energy and Fuels, 21/1.

Mora-Vergara, I. D., Hernández Moscoso, L., Gaigneaux, E. M., Giraldo, S. A., and Baldovino-Medrano, V. G. (2018). Hydrodeoxygenation of guaiacol using NiMo and CoMo catalysts supported on alumina modified with potassium. Catalysis Today, 302, 125–135.

Pattanaik, B. P., and Misra, R. D. (2017). Effect of reaction pathway and operating parameters on the deoxygenation of vegetable oils to produce diesel range hydrocarbon fuels: A review. Renewable and Sustainable Energy Reviews, 73, 545–557.

Rashidi, N. A., Mustapha, E., Theng, Y. Y., Razak, N. A. A., Bar, N. A., Baharudin, K. B., and Derawi, D. (2022). Advanced biofuels from waste cooking oil via solventless and hydrogen-free catalytic deoxygenation over mesostructured Ni-Co/SBA-15, Ni-Fe/SBA-15, and Co-Fe/SBA-15 catalysts. Fuel, 313, 122695.

Reid, W. V., Ali, M. K., and Field, C. B. (2020). The future of bioenergy. Global Change Biology, 26/1, 274–286.

Review, E. P. (2021). Turkey 2021. IEA (2021), Turkey 2021 Energy Policy Review, IEA Energy Policy Reviews, OECD Publishing, Paris,.

Ritchie, Hannah; Roser, M. (2018). Fossil Fuels; Our world in data. In Our world in data.

Rogers, K. A., and Zheng, Y. (2016). Selective Deoxygenation of Biomass-Derived Bio-oils within Hydrogen-Modest Environments:AReview and New Insights.

Roh, H. S., Eum, I. H., Jeong, D. W., Yi, B. E., Na, J. G., and Ko, C. H. (2011). The effect of calcination temperature on the performance of Ni/MgO–Al2O3 catalysts for decarboxylation of oleic acid. Catalysis Today, 164/1, 457–460.

Safa Gamal, M., Asikin-Mijan, N., Arumugam, M., Rashid, U., and Taufiq-Yap, Y. H. (2019). Solvent-free catalytic deoxygenation of palm fatty acid distillate over cobalt and manganese supported on activated carbon originating from waste coconut shell. Journal of Analytical and Applied Pyrolysis, 144, 104690.

Santillan-Jimenez, E., and Crocker, M. (2012). Mini-review Catalytic deoxygenation of fatty acids and their derivatives to hydrocarbon fuels via decarboxylation/decarbonylation. Wileyonlinelibrary.Com).

Sari, E., Kim, M., Salley, S. O., and Ng, K. Y. S. (2013). A highly active nanocomposite silica-carbon supported palladium catalyst for decarboxylation of free fatty acids for green diesel production: Correlation of activity and catalyst properties. Applied Catalysis A: General, 467, 261–269.

Simakova, I., Simakova, O., Mäki-Arvela, P., and Murzin, D. Y. (2010). Decarboxylation of fatty acids over Pd supported on mesoporous carbon. Catalysis Today, 150/1–2, 28–31.

Tran, N. T. T., Uemura, Y., Chowdhury, S., and Ramli, A. (2016). Vapor-phase hydrodeoxygenation of guaiacol on Al-MCM-41 supported Ni and Co catalysts. Applied Catalysis A: General, 512, 93–100.

Tran, Q. K., Ly, H. V., Kwon, B., Kim, S. S., and Kim, J. (2021). Catalytic hydrodeoxygenation of guaiacol as a model compound of woody bio-oil over Fe/AC and Ni/γ-Al2O3 catalysts. Renewable Energy, 173, 886–895.

Wang, F., Jiang, J., Wang, K., Zhai, Q., Sun, H., Liu, P., Feng, J., Xia, H., Ye, J., Li, Z., Li, F., and Xu, J. (2018). Activated carbon supported molybdenum and tungsten carbides for hydrotreatment of fatty acids into green diesel. Fuel, 228, 103–111.

Wang, F., Xu, J., Jiang, J., Liu, P., Li, F., Ye, J., and Zhou, M. (2018). Hydrotreatment of vegetable oil for green diesel over activated carbon supported molybdenum carbide catalyst. Fuel, 216, 738–746.

Wang, H., Rogers, K., Zhang, H., Li, G., Pu, J., Zheng, H., Lin, H., Zheng, Y., and Ng, S. (2019). The effects of catalyst support and temperature on the hydrotreating of waste cooking oil (WCO) over CoMo sulfided catalysts. Catalysts, 9/8.

Yeletsky, P. M., Kukushkin, R. G., Yakovlev, V. A., and Chen, B. H. (2020). Recent advances in one-stage conversion of lipid-based biomass-derived oils into fuel components – aromatics and isomerized alkanes. Fuel, 278, 118255.

Yoon, J. J. (2009). What's the Difference between Biodiesel and Renewable (Green) Diesel. In Advanced Biofuels USA (pp. 1–14).

Zhang, H., Fu, S., Du, X., and Deng, Y. (2021). Advances in Versatile Nanoscale Catalyst for the Reductive Catalytic Fractionation of Lignin. ChemSusChem, 14, 2268–2294.

Zhang, Z., Tang, M., and Chen, J. (2016). Effects of P/Ni ratio and Ni content on performance of γ-Al2O3-supported nickel phosphides for deoxygenation of methyl laurate to hydrocarbons. Applied Surface Science, 360, 353–364.

APPENDIX

Appendix A. Materials & Streams Report

OVERALL PROCESS DATA

Annual Operating Time	7,920.00 h
Unit Production Ref. Rate	2,590,723.57 kg MP
Batch Size	790.58 kg MP
Recipe Batch Time	3.00 h
Recipe Cycle Time	2.42 h
Number of Batches per Year	3,277.00

OVERALL COMPONENT BALANCE (kg/batch)

COMPONENT	INITIAL	INPUT	OUTPUT	FINAL	IN-OUT
Catalyst	0.000	50.000	50.000	0.000	0.000
Nitrogen	2.928	0.007	0.005	2.930	0.000
Oleic Acid	0.000	883.604	883.604	0.000	0.000
Oxygen	0.889	0.000	0.002	0.887	0.000
TOTAL	3.817	933.610	933.611	3.817	0.000

EQUIPMENT CONTENTS

R-101

Procedure	Operation	Time (in h)	Volume (in L)
P-6	START	0.000	0.000
P-6	CHARGE-1 (Charge)	0.333	0.000
P-6	REACT-1 (Batch Stoich. Reaction)	2.083	1,005.654
P-6	TRANSFER-OUT-1 (Transfer Out)	2.417	0.000

V-102

Procedure	Operation	Time (in h)	Volume (in L)
P-9	START	2.417	0.000
P-9	TRANSFER-IN-1 (Transfer In)	2.750	907.869
P-9	HOLD-1 (Holding)	3.000	907.869
P-9	END	3.000	0.000

TNK-101

Procedure	Operation	Time (in h)	Volume (in L)
P-2	START	0.000	0.000
P-2	TRANSFER-IN-1 (Transfer In)	0.333	1,000.019
P-2	HOLD-1 (Holding)	0.417	1,000.019
P-2	END	0.417	0.000

Appendix B. Economic Evaluation Report

LABOR COST - PROCESS SUMMARY

Labor Type	**Unit Cost ($/h)**	**Annual Amount (h)**	**Annual Cost ($)**	**%**
Operator	2.88	49,883	143,414	25.90
QC Analyst	3.22	34,135	109,916	19.85
Supervisor	4.20	34,135	143,369	25.89
Reactor Operator	4.60	34,135	157,023	28.36
TOTAL		152,289	553,722	100.00

MATERIALS COST - PROCESS SUMMARY

Bulk Material	**Unit Cost ($)**	**Annual Amount**		**Annual Cost ($)**	**%**
Catalyst	0.500	163,850	kg	81,925	3.22
Nitrogen	3.000	23	kg	68	0.00
Oleic Acid	0.850	2,895,569	kg	2,461,234	96.78
TOTAL				2,543,226	100.00

NOTE: Bulk material consumption amount includes material used as:
- Raw Material
- Cleaning Agent
- Heat Transfer Agent (if utilities are included in the operating cost)

Appendix C. Cash Flow Analysis Report

CASH FLOW ANALYSIS (thousand $)

Year	**Capital Investment**	**Debt Finance**	**Sales Revenues**	**Operating Cost**	**Gross Profit**	**Loan Payments**	**Depreciation**	**Taxable Income**	**Taxes**	**Net Profit**	**Net Cash Flow**
1	- 78	0	0	0	0	0	0	0	0	0	- 78
2	- 416	0	984	1,321	- 337	0	25	0	0	- 313	- 729
3	- 78	0	3,935	3,476	460	0	25	460	161	324	245
4	0	0	3,935	3,476	460	0	25	460	161	324	324
5	0	0	3,935	3,476	460	0	25	460	161	324	324
6	0	0	3,935	3,476	460	0	25	460	161	324	324
7	0	0	3,935	3,476	460	0	25	460	161	324	324
8	0	0	3,935	3,476	460	0	25	460	161	324	324
9	0	0	3,935	3,476	460	0	25	460	161	324	324
10	0	0	3,935	3,476	460	0	25	460	161	324	324
11	0	0	3,935	3,476	460	0	25	460	161	324	324
12	0	0	3,935	3,451	485	0	0	485	170	315	315
13	0	0	3,935	3,451	485	0	0	485	170	315	315
14	0	0	3,935	3,451	485	0	0	485	170	315	315
15	325	0	3,935	3,451	485	0	0	485	170	315	639

IRR/NPV SUMMARY

IRR Before Taxes	53.67 %	Interest %	7.00	9.00	11.00
IRR After Taxes	35.70 %	NPV	1,811.00	1,495.00	1,235.00

BREAKDOWN OF CAPITAL OUTLAY ($)

Year	Direct Fixed Capital	Working Capital	Start-Up Cost	Up Front R&D	Up Front Royalties	Total
1	- 78,448	0	0	0	0	- 78,448
2	- 104,597	- 311,461	- 13,075	0	0	- 416,058
3	- 78,448	0	0	0	0	- 78,448
4	0	0	0	0	0	0
5	0	0	0	0	0	0
6	0	0	0	0	0	0
7	0	0	0	0	0	0
8	0	0	0	0	0	0
9	0	0	0	0	0	0
10	0	0	0	0	0	0
11	0	0	0	0	0	0
12	0	0	0	0	0	0
13	0	0	0	0	0	0
14	0	0	0	0	0	0
15	13,075	311,461	0	0	0	324,535

Appendix D. Equipment Gantt Chart (for single batch)

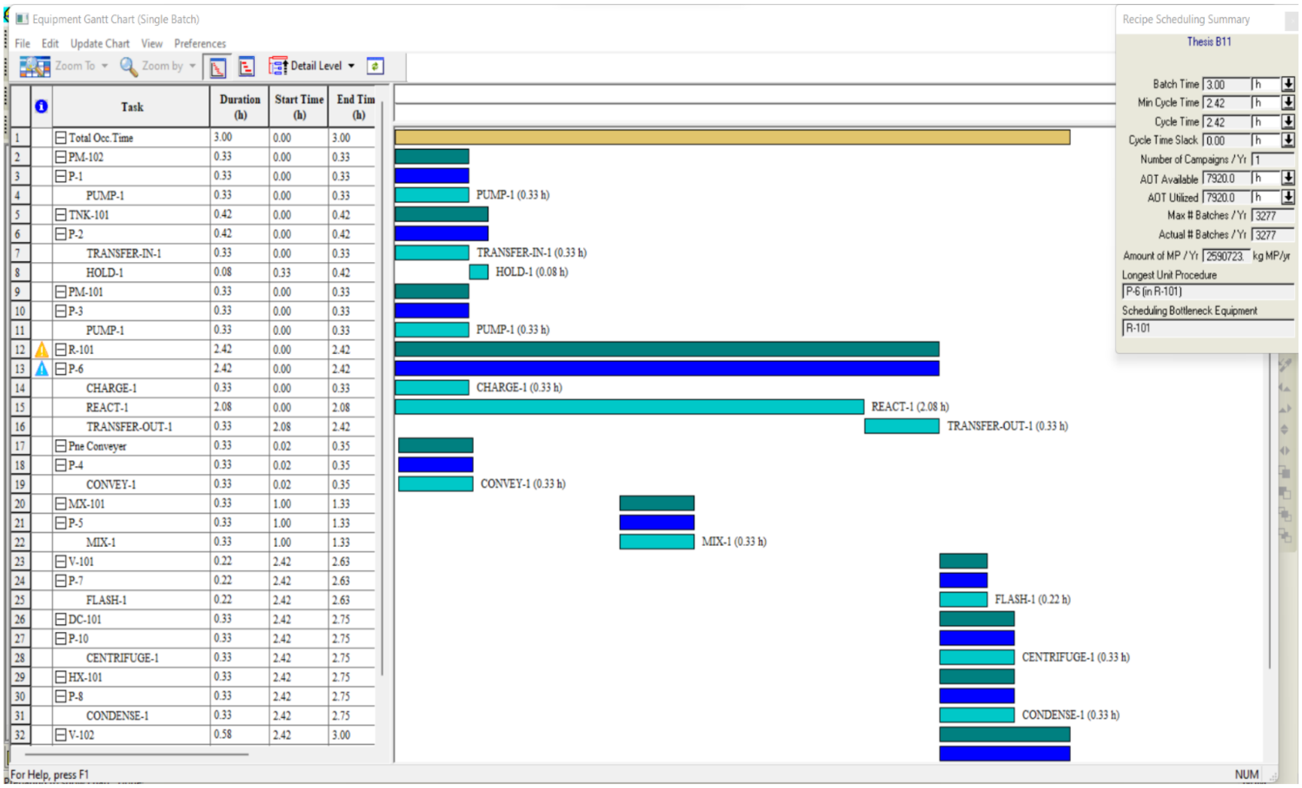

	ℹ	Task	Duration (h)	Start Time (h)	End Tim (h)
1		⊟ Total Occ.Time	3.00	0.00	3.00
2		⊟ PM-102	0.33	0.00	0.33
3		⊟ P-1	0.33	0.00	0.33
4		PUMP-1	0.33	0.00	0.33
5		⊟ TNK-101	0.42	0.00	0.42
6		⊟ P-2	0.42	0.00	0.42
7		TRANSFER-IN-1	0.33	0.00	0.33
8		HOLD-1	0.08	0.33	0.42
9		⊟ PM-101	0.33	0.00	0.33
10		⊟ P-3	0.33	0.00	0.33
11		PUMP-1	0.33	0.00	0.33
12	⚠	⊟ R-101	2.42	0.00	2.42
13	⚠	⊟ P-6	2.42	0.00	2.42
14		CHARGE-1	0.33	0.00	0.33
15		REACT-1	2.08	0.00	2.08
16		TRANSFER-OUT-1	0.33	2.08	2.42
17		⊟ Pne Conveyer	0.33	0.02	0.35
18		⊟ P-4	0.33	0.02	0.35
19		CONVEY-1	0.33	0.02	0.35
20		⊟ MX-101	0.33	1.00	1.33
21		⊟ P-5	0.33	1.00	1.33
22		MIX-1	0.33	1.00	1.33
23		⊟ V-101	0.22	2.42	2.63
24		⊟ P-7	0.22	2.42	2.63
25		FLASH-1	0.22	2.42	2.63
26		⊟ DC-101	0.33	2.42	2.75
27		⊟ P-10	0.33	2.42	2.75
28		CENTRIFUGE-1	0.33	2.42	2.75
29		⊟ HX-101	0.33	2.42	2.75
30		⊟ P-8	0.33	2.42	2.75
31		CONDENSE-1	0.33	2.42	2.75
32		⊟ V-102	0.58	2.42	3.00

Recipe Scheduling Summary

Thesis B11

Batch Time 3.00 h
Min Cycle Time 2.42 h
Cycle Time 2.42 h
Cycle Time Slack 0.00 h
Number of Campaigns / Yr 1
AOT Available 7920.0 h
AOT Utilized 7920.0 h
Max # Batches / Yr 3277
Actual # Batches / Yr 3277
Amount of MP / Yr 2590723. kg MP/yr
Longest Unit Procedure P-6 (in R-101)
Scheduling Bottleneck Equipment R-101

Equipment Gantt Chart (for single batch)

Appendix E. Some Laboratory Activities

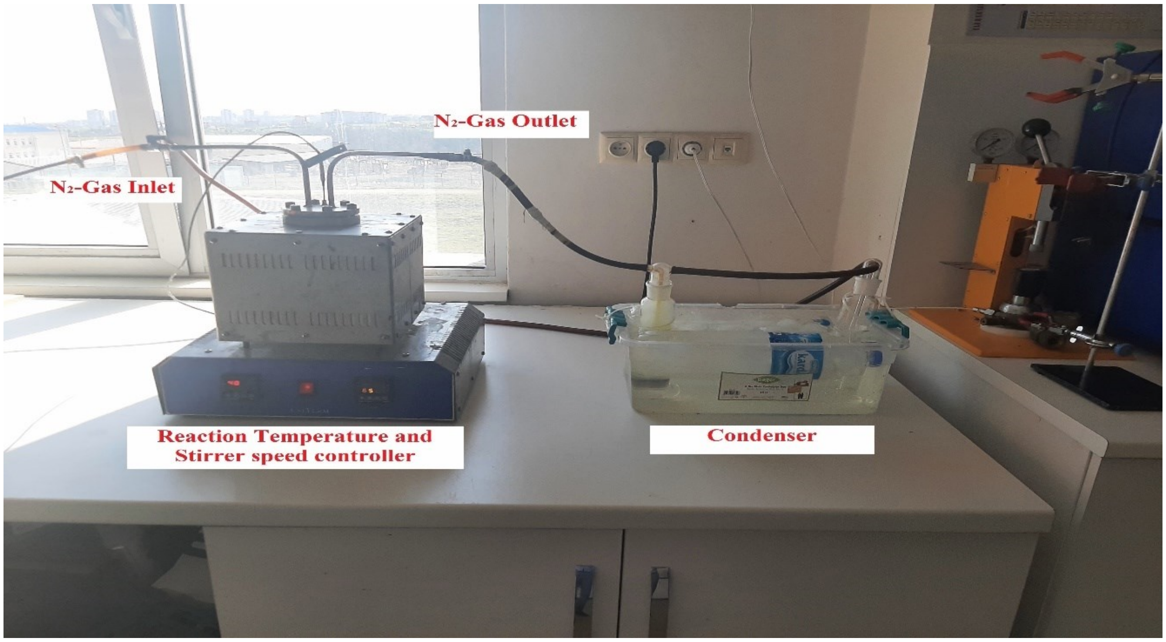

During the Calcination process

Measuring the sample heating value by using oxygen bomb calorimeter

CURRICULUM VITAE

Mohammed Siraj ESHETEA completed high school education at Debre Birhan Secondary School and Haile Mariam Mamo preparatory school, Ethiopia, in 2011. In 2016, he graduated with a BSc degree in Chemical Engineering from Adama Science and Technology University. He has 1 and a half years of work experience as a production assistant in the SilAfrica Plastic and Chemical industry PLC (2017 - 2018), Ethiopia. After 1 and a half years of work experience as an Academic and Research Assistant in the Department of Chemical Engineering at Adama Science and Technology University (2018 - 2019), he won a Turkish scholarship and pursued his MSc studies in Turkey.

Languages

Amharic	Native
English	C1
Turkish	C1

Work Experience

- ⇒ Academic and Research Assistant in the Department of Chemical Engineering, Adama Science and Technology University (2018 - 2019), Ethiopia.
- ⇒ Production assistant in the SilAfrica Plastic and Chemical industry PLC (2017 - 2018), Ethiopia.

Computer Skills

- ⇒ Aspen Plus, Chemcad, and Super Pro Desıgn
- ⇒ Mıcrosoft Office (Excel, Word, Power Point…)

Personal information:

ORCID ID: 0000-0002-0637-7074

Publications:

1. Siraj, M.S., and Ceylan, S. (2022). Catalytic deoxygenation of oleic acid over CoMo/Zeolite Catalyst for green diesel production. Anadolu Journal of Bioenergy Studies (Forthcoming in 2022).